Transportation Research Part E 97 (2017) 69–96

Contents lists available at ScienceDirect

Transportation Research Part E

journal homepage: www.elsevier.com/locate/tre

# Bulk ship fleet renewal and deployment under uncertainty: A multi-stage stochastic programming approach

Ayşe N. Arslan [a], Dimitri J. Papageorgiou [b,*]

[a] Department of Industrial & Systems Engineering, University of Florida, Gainesville, FL 32611, USA
[b] Corporate Strategic Research, ExxonMobil Research and Engineering Company, 1545 Route 22 East, Annandale, NJ 08801, USA

ARTICLE INFO

*Article history:*
Received 20 December 2015
Received in revised form 18 September 2016
Accepted 19 October 2016
Available online 17 November 2016

*Keywords:*
Chartering
Fleet planning
Fleet renewal
Maritime transportation
Mixed-integer linear programming
Multi-stage stochastic programming

ABSTRACT

Faced with simultaneous demand and charter cost uncertainty, an industrial shipping company must determine a suitable fleet size, mix, and deployment strategy to satisfy demand. It acquires vessels by time chartering and voyage chartering. Time chartered vessels are acquired for different durations, a decision made before stochastic parameters are known. Voyage charters are procured for a single voyage after uncertain parameters are realized. We introduce the first multi-stage stochastic programming model for the bulk ship fleet renewal problem and solve it in a rolling horizon fashion. Computational results indicate that our approach outperforms traditional methods relying on expected value forecasts.


## 1. Introduction

This paper investigates a multi-period maritime fleet sizing and deployment problem with uncertain customer demand and charter costs. An industrial bulk shipper, whose primary task is to transport raw materials produced or owned by a parent company from supply ports to demand ports, must determine the number of each vessel type and the fleet deployment strategy needed to reliably satisfy stochastic demand at minimum cost. A major challenge in constructing an appropriate fleet is the prevalence of severe market fluctuations in the maritime sector, where unpredictable shipping cycles are the norm, not the exception (Stopford, 2008).

Despite the recognition of significant uncertainty in the maritime sector, decision support tools that explicitly account for stochasticity are scarce (Pantuso et al., 2014a). Those models that do consider uncertainty focus almost exclusively on liner shipping applications and/or strategic planning problems with long planning horizons (on the order of a decade). In contrast, this work investigates a problem in bulk shipping and offers a model that can be used for tactical planning or for planning at the interface of the strategic and tactical level. Specifically, we consider a fleet sizing and deployment problem faced by a bulk shipper who operates a heterogeneous fleet composed of company-owned vessels as well as time and voyage chartered vessels. Every few months, prior to observing actual demand and future charter rates, the shipper determines how many time charter vessels to acquire and the charter duration for each vessel. Purchasing new vessels is not considered in this work. The planning horizon of interest is typically six months to three years with a time period representing three or six months. After demand in the current period is realized, the shipper must deploy her fleet to satisfy demand. If too few time

* Corresponding author.
*E-mail addresses:* nur.arslan@ufl.edu (A.N. Arslan), dimitri.j.papageorgiou@exxonmobil.com (D.J. Papageorgiou).

http://dx.doi.org/10.1016/j.tre.2016.10.009
1366-5545/

**Nomenclature**

*Indices and sets*

| | |
|---|---|
| $t \in \mathcal{T}$ | set of time periods of the planning horizon with $T = \lvert\mathcal{T}\rvert$ |
| $l \in \mathcal{L}$ | set of loading ports with $L = \lvert\mathcal{L}\rvert$ |
| $d \in \mathcal{D}$ | set of discharging ports with $D = \lvert\mathcal{D}\rvert$ |
| $j \in \mathcal{J}$ | set of all ports: $\mathcal{J} = \mathcal{L} \cup \mathcal{D}$ |
| $p \in \mathcal{P}$ | set of vessel paths (sequences of port calls) |
| $p \in \mathcal{P}_l^{\text{Origin}}$ | set of paths that have loading port $l$ as origin |
| $p \in \mathcal{P}_l$ | set of paths that include loading port $l$ as a port call |
| $p \in \mathcal{P}_d$ | set of paths that include discharging port $d$ as a port call |
| $vc \in \mathcal{VC}$ | set of vessel classes with $VC = \lvert\mathcal{VC}\rvert$ |
| $f \in \mathcal{F}_{vc}$ | set of fare classes for a vessel class $vc$ |
| $k \in \mathcal{K}$ | set of vessel types: $\mathcal{K} = \{\text{Owned}, \text{Time Chartered (TC)}, \text{Voyage Chartered (VC)}\}$ |
| $k \in \mathcal{K}'$ | subset of vessel types: $\mathcal{K}' = \{\text{Owned}, \text{Time Chartered (TC)}\}$ |

*Deterministic parameters*

| | |
|---|---|
| $\overline{T}$ | duration in days of each time period |
| $M_{vc,f}$ | number of vessels in vessel class $vc$ that can be chartered from fare class $f$ |
| $P_{l,t}$ | production limit at loading port $l$ in time period $t$ |
| $Q_{vc}$ | capacity of a vessel in vessel class $vc$ |
| $\overline{Q}_{vc,p,j}$ | amount of product loaded or discharged at port $j$ from a vessel in vessel class $vc$ on path $p$ |
| $D_{p,vc,t}$ | time required to complete path $p$ with vessel class $vc$ beginning in time period $t$ |
| $\overline{S}_{d,t}$ | maximum amount of inventory that can be stored at discharging port $d$ in time period $t$ |
| $C^{\text{V+O}}_{p,vc,k,t}$ | voyage and operating cost of deploying a type $k \in \mathcal{K}'$ vessel in vessel class $vc$ on a voyage on path $p$ beginning in time period $t$ |
| $C^{\text{Repo}}_{l,l',vc,k,t}$ | repositioning cost associated with reassigning a type $k \in \mathcal{K}'$ vessel in vessel class $vc$ from loading port $l$ to loading port $l'$ at the beginning of time period $t$ |

*Stochastic parameters*

| | |
|---|---|
| $\widetilde{\Delta}_{d,t}$ | demand at discharging port $d$ in time period $t$ |
| $\widetilde{C}^{\text{TC}}_{l,vc,f,t_1,t_2}$ | time charter cost for a vessel in vessel class $vc$ and fare class $f$ based in loading port $l$ for chartering at the end of time period $t_1$ until the end of time period $t_2$ |
| $\widetilde{C}^{\text{VC}}_{p,vc,t}$ | voyage charter rate for a vessel in vessel class $vc$ serving path $p$ in time period $t$ |

*Decision variables*

| | |
|---|---|
| $x^{\text{TC}}_{l,vc,f,t_1,t_2}$ | (integer) number of time chartered vessels initially based in loading port $l$, in vessel class $vc$ and fare class $f$, chartered at the end of time period $t_1$ until the end of time period $t_2$ |
| $y^{\text{TC,Exit}}_{l,vc,t}$ | (integer) number of time chartered vessels in vessel class $vc$ exiting the fleet at the end of time period $t$ from loading port $l$ |
| $y^{\text{Repo}}_{l,l',vc,k,t}$ | (integer) number of type $k \in \mathcal{K}'$ vessels in vessel class $vc$ repositioned from loading port $l$ to loading port $l'$ at the beginning of time period $t$ |
| $y_{l,vc,k,t}$ | (integer) number of type $k \in \mathcal{K}'$ vessels in vessel class $vc$ assigned to loading port $l$ for the duration of time period $t$ after repositioning decisions have been made |
| $z_{p,vc,k,t}$ | (continuous) number of trips made on path $p$ using type $k \in \mathcal{K}$ vessels of class $vc$ during time period $t$ |
| $s_{d,t}$ | (continuous) inventory level at discharging port $d$ at the end of time period $t$ |

charter vessels are available, voyage charter vessels can be procured, each making a single voyage from a supply port to a demand port to fulfill remaining demand.

Amidst all of the complexity, the heart of this problem is to find an optimal balance of long-term time charter commitments and short-term voyage charter acquisitions on a recurring basis. With perfect demand and cost foresight, the shipper could construct her fleet rather easily by solving a deterministic optimization problem to identify the most cost effective vessels to acquire. The problem is that market cycles and demand can be difficult to predict. Consequently, "when trade is buoyant and voyage rates are rising, charterers, in anticipation of further rises, tend to charter for longer periods to cover their commitments; when rates are expected to fall, they tend to contract for shorter periods" (Branch, 2007, p. 194).

Several types of chartering are traditionally used in the shipping industry. Akin to leasing a car, a time charter is the hiring of a vessel for a specific time interval, typically on the order of months to years. The vessel owner manages the vessel, while the charterer dictates the vessel's schedule. The charterer pays for all bunker fuel costs, port fees, commissions, and a daily hire to the vessel owner. In contrast, a voyage charter is more analogous to a taxi service in which a vessel and its crew are hired for a single voyage. The charterer pays the vessel owner a lump sum (possibly with additional payments such as demurrage, a charge payable to the owner of a chartered ship in respect of failure to load or discharge the ship within the time agreed, or those negotiated in a contract). Meanwhile, the vessel owner pays the fuel costs, port fees, and crew costs. In general, time and voyage charter rates move in the same direction, i.e., are highly positively correlated, but because time charter rates depend on market expectations, they tend to fluctuate more widely than voyage rates (Branch, 2007).

A distinguishing characteristic of this paper is that time charter durations are treated as decision variables to be optimized. To the best of our knowledge, existing models in the literature do not explicitly include the duration of fleet acquisition decisions, e.g., vessel purchasing decisions or charter-in decisions. The fact that time charter vessels can be procured for different durations of time offers the shipper an additional mechanism to hedge against uncertain market conditions. For example, if the shipper believes that demand will increase over the next year or two, she will likely time charter for longer durations as time charter rates typically reflect current market trends more so than market forecasts, i.e., current time charter rates are likely to be lower than those in the future. On the other hand, if demand is projected to diminish, she may choose to time charter for shorter durations in anticipation that future rates will fall. In some circumstances, however, low demand reflects a reduction in global demand, which in turn drives voyage rates very low relative to time charter rates. It is in these times when a shipper with many time chartered vessels finds her fleet significantly under-utilized.

In a broader sense, this research addresses the fleet sizing and mix problem in maritime applications, which usually falls under the larger umbrella of strategic planning, and typically includes decisions related to capacity expansion for future demand growth, technology upgrades for improving operations, and contractual agreements between suppliers and consumers. When vehicle allocation and deployment issues are also considered, the problem becomes more tactical in nature. In the maritime sector, fleet planning models traditionally involve horizons of multiple years, even decades, to help decision-makers with purchasing decisions for new vessels. In this paper, we focus on a medium-term problem that lies at the boundary of strategic and tactical problems. Although the vessel procurement decisions are the primary concern, it is important for the shipper to also consider how vessels will be deployed after being procured. In reality, vessel deployment can be rather complicated. Given a fixed fleet, our problem could be formulated as a stochastic maritime inventory routing problem which, at a tactical level, can be very challenging to solve even when the problem is fully deterministic (Papageorgiou et al., 2014). Thus, to make the problem more computationally tractable, we do not make detailed routing decisions, but instead assign time chartered vessels to cyclic routes as explained in Section 2.

### 1.1. Literature review

Fleet sizing, planning, and deployment problems are ubiquitous in the transportation sector. Hoff et al. (2010) present a literature survey on fleet composition and routing problems arising in maritime and road-based settings. Bojović and Milenkovic (2008) discusses several models in the rail sector literature. Pantuso et al. (2014a) provide a survey on the fleet size and mix problem focused exclusively on the maritime sector. The idiosyncrasies of maritime transportation are highlighted in Christiansen et al. (2007) and Hoff et al. (2010). To avoid significant overlap with the review given in Pantuso et al. (2014a), this section emphasizes prior research on maritime fleet sizing and deployment that explicitly treats uncertainty in the associated mathematical models and solution framework. Table 1, adapted from Pantuso et al. (2014a) and extended to our setting, attempts to categorize these papers. We also mention several papers within the petrochemical sector, the application domain that inspired this work. Additional discussion of the interaction between fleet sizing and ship routing and scheduling is given in Christiansen et al. (2013).

As this paper concerns industrial bulk shipping, i.e., a setting in which companies ship their own goods using their own fleet, we begin with prior research tailored to this segment of the shipping sector. Alvarez et al. (2011) study a strategic fleet sizing and deployment problem for bulk shippers and develop a robust optimization model to handle random parameters. While their model considers uncertainty in numerous parameters, their case study only considers uncertainty in a subset of objective function coefficients including purchase prices, sale prices, sunset values, and charter rates. Right-hand side parameters and matrix coefficients are deterministic. Compared to our problem, they consider a longer planning horizon with more decisions such as purchasing and sales options. Their deployment decisions are less complicated than ours.

Another stream of stochastic fleet sizing research has emerged to aid the liner (container) shipping community. Liner shipping resembles bus line operations where companies deploy their vessels according to pre-published schedules on fixed itineraries. Meng and Wang (2010) present a short-term (one-year) single-period fleet planning problem with demand uncertainty along liner service routes. The aim is to determine a short-term (36 months) joint ship fleet design and deployment plan. They formulate the problem as a chance-constrained mixed-integer program (MIP) before re-casting it as a pure MIP by exploiting their assumption that cargo shipment demand between any two ports on each liner service route is normally distributed. This work is extended in Meng et al. (2012) in several ways. First, they consider container transshipment, an important and common operation in liner shipping that allows consolidation of goods and, in turn, larger vessels to be used. They develop a two-stage stochastic mixed-integer programming model to help decide the number and type of vessels to use prior to realizing demand. These two papers are tailored to a tactical planning problem, assume one form of chartering

**Table 1**
(Adapted from Pantuso et al. (2014a).) A dash (–) implies that this item was not specified. Problem category: LSFP = liner ship fleet planning; MFSMP = maritime fleet size and renewal problem; SFRPS = strategic fleet renewal problem in shipping; Acquisition/disposal: B = build; CI = charter in; CO = charter out; CP = choose from a pool; LU = lay up; P = purchase; SC = scrapping; SE = sale; SH = buy in the second-hand marked. Mode: IN = industrial; LI = liner; TR = tramp. Methodology: RO = robust optimization; SIM = simulation; StP = stochastic programming. Operating decisions: D = deployment: number of vessels assigned to each pre-determined route; R = routing: sequence of port visits; S = scheduling: routing + assigning a time to each port call. Type of chartering: time charter = charterer pays for all fuel the vessel consumes, port charges, commissions, and a daily hire; voyage charter = charterer pays the vessel owner on a lump-sum basis while the vessel owner pays the port fees, fuel costs, and crew costs. Bareboat = charterer manages the vessel and pays all costs except the capital repayment, tax, and depreciation. Time horizon (# of periods): maximum time interval (number of time periods) reported in a given solve.

| Authors | Problem category | Planning level | Acquisition/ disposal | Mode | Industry | Method-ology | Operating decisions | Type of chartering | Time horizon (# of periods) |
|---|---|---|---|---|---|---|---|---|---|
| Alvarez et al. (2011) | SFRPS | Strategic | P,CI,CO, SE, SC,LU | TR or IN | Bulk | RO | D | Time, Voyage | 8 years (32) |
| Bakkehaug et al. (2014) | SFRPS | Strategic | P,CI,CO,SE,SC | LI | Ro-ro | StP | D | – | 15 years (8[a]) |
| Fagerholt et al. (2010) | SFRPS | Strategic | – | TR or IN | General | SIM | R + S | – | 1 year (52) |
| Meng and Wang (2010) | LSFP | Tactical | CP,CI,CO | LI | Container | StP | D | Bareboat | 1 year (1) |
| Meng and Wang (2011) | LSFP | Strategic | P,CI,CO,SE | LI | Container | DP | D | – | 10 years (10) |
| Meng et al. (2012) | LSFP | Tactical | CP,CI,CO | LI | Container | StP | D | Bareboat | 3–6 months (1) |
| Meng et al. (2015) | LSFP | Strategic | P,CI,CO,SE | LI | Container | StP | D | – | 10 years (10) |
| Pantuso et al. (2014b) | SFRPS | Strategic | B,CI,CO,LU, SC,SE,SH | LI | Container | StP | D | Time, Voyage | 6 years (4) |
| Pantuso et al. (2016) | SFRPS | Strategic | B,CI,CO,LU, SC,SE,SH | LI | Container | StP | D | Time, Voyage | 6 years (4) |
| Shyshou et al. (2010) | MFSMP | Tactical | CI | IN | Offshore services | SIM | – | Voyage | 1 year (1) |
| This paper | MFSMP | Tactical | CI | IN | Bulk | StP | D | Time, Voyage | 1–5 years (12) |

[a] Bakkehaug et al. (2014) run simulations with a 15 year horizon, while the maximum number of periods considered in their stochastic program is 8.

(bareboat chartering), and only consider a single planning period. Meng et al. (2015) extend this work to a strategic and multi-period problem by incorporating random and period-dependent container shipment demand. Meng et al. (2012, 2015) propose two solution methods, with dual decomposition and Lagrangian relaxation at the core, to solve these problems. Finally, we note that Meng and Wang (2011) also studied a multi-period fleet planning problem and used a scenario tree approach. However, this problem had no uncertain parameters.

Pantuso et al. (2014b) study a maritime fleet renewal problem (MFRP) in which a decision-maker must decide how to modify its current fleet in order to efficiently meet future market requirements. The shipping company must decide how many vessels of each type to include in the current fleet or dispose of, when and how to do so. The fleet can be expanded by ordering newbuildings or purchasing second-hand ships, and scaled down by selling or demolishing (scrapping) ships. The delivery time for newbuildings is in general longer than for second-hand ships. Their case study is tailored to a real world application with Wallenius Wilhelmsen Logistics, a major liner shipper of rolling equipment. Their problem is formulated as a multi-stage stochastic program, which can be transformed into a two-stage stochastic MIP (with continuous recourse), and is solved via a decomposition coupling tabu search (for the master problem) and linear programming (for the subproblems). Pantuso et al. (2016) address a similar fleet renewal problem and show that solutions obtained from their stochastic model perform noticeably better than solutions obtained using average values.

Bakkehaug et al. (2014) study what they term the strategic fleet renewal problem in shipping (SFRPS) in which a shipping company must repeatedly adjust its vessel fleet to meet uncertain future transportation demands and compensate for aging vessels. Their model, a multi-stage stochastic program, explicitly captures uncertainty in fourteen parameters, including both objective function and right hand side parameters. They perform extensive computational experiments to compare different scenario tree structures to represent realizations of uncertain parameters. The model and solutions generated are evaluated within a rolling-horizon framework where significantly better results are obtained from their stochastic model compared to using an expected value approach.

The papers discussed thus far have all applied mathematical programming techniques, e.g., stochastic programming or robust optimization, to explicitly account for parameter uncertainty within a mathematical model. Another line of research makes use of simulation techniques to evaluate and optimize fleet planning decisions. Though generally confined to problems with a smaller number of potential fleet size configurations, simulation often offers a more detailed representation of uncertainty. In practice, this additional detail can be a useful tool when trying to convince management of the benefits of decision support tools that go beyond traditional spreadsheet planning.

Fagerholt et al. (2010) present a methodology that combines simulation and optimization, where a Monte Carlo simulation framework is built around an optimization-based decision support system for short-term routing and scheduling. The simulation solves a series of short-term routing and scheduling problems, each dependent on realizations of uncertain parameters, within a rolling horizon framework. Fagerholt and Rygh (2002) employed simulation to aid in the design of a sea-borne fresh water transport system from Turkey to Jordan. The associated decision support tool was used to determine the required number, capacity, and speed of vessels, as well as a number of other design factors. Halvorsen-Weare and Fagerholt (2011) applied simulation, in combination with their deterministic optimization model developed in Halvorsen-Weare et al. (2012), to determine more robust schedules within a larger decision support system for fleet planning and weekly ship scheduling. The uncertainty was restricted to random weather conditions that affected weekly schedules as opposed to long-term cost and demand parameters that typically arise in strategic and tactical planning. Shyshou et al. (2010) developed a discrete-event simulation model to evaluate alternative fleet size configurations for anchor handling operations in a project initiated by StatoilHydro, the largest Norwegian offshore oil and gas operator. Similar to the chartering options in our paper, their study investigated the trade-off between hiring vessels either on the long-term basis or on the spot market (where spot rates are frequently a magnitude higher than long-term rates).

In addition to the work of Shyshou et al. (2010), there are several notable applications of fleet sizing in the petrochemical sector. Cheon et al. (2012) study a railcar fleet sizing problem in the chemical industry in which railcars are used for storage and transportation. They cast their problem as a long-term capacity expansion problem and solve it using mixed-integer linear programming techniques. Singer et al. (2002) discuss an application with stochastic demand in the distribution of liquefied petroleum gas. In their problem, trucks are dispatched without knowing actual demand and must react en route as demands are realized. Finally, List et al. (2003) present a sector-independent two-stage stochastic programming formulation and stochastic decomposition algorithm for fleet sizing under uncertain demand and operating conditions.

### *1.2. Contributions of this paper*

As mentioned above, there is a dearth of decision support tools in the maritime sector that explicitly account for parameter uncertainty (Pantuso et al., 2014a). In the existing models that consider stochastic maritime fleet sizing, the emphasis is on container shipping and/or strategic planning problems where vessel purchasing decisions are the primary concern. Moreover, these models cannot be immediately adapted to our setting since the associated strategic decisions and ship deployment characteristics are sufficiently different in container shipping. For these reasons, we explore a problem in industrial bulk shipping and provide a stochastic programming model that can be used for tactical planning or for planning at the interface of the strategic and tactical level.

The contributions of this paper are:

1. The first multi-stage stochastic programming approach to tactical fleet renewal and deployment for industrial bulk shipping.
2. The first mathematical optimization model for bulk ship fleet renewal to treat time charter durations as a decision variable.
3. A model that explicitly considers demand and charter cost uncertainty, and therefore addresses an area in need of additional research as put forth in Christiansen et al. (2007) and Pantuso et al. (2014a).
4. An investigation of the benefits of using different scenario tree representations and including alternate recourse decisions in the formulation when the predicted market condition does and does not match the actual market condition.
5. Empirical evidence that making chartering decisions based on a stochastic programming look-ahead model can result in as much as a 12% average cost reduction relative to using a deterministic look-ahead.

The remainder of the paper is organized as follows: Section 2 describes the problem characteristics and a mathematical formulation to model it. In Section 3, a look-ahead model is presented along with the three solution methods compared in our computational experiments section. In Section 4, a base instance and scenario generation procedure is outlined. Section 5 describes the experiments designed to test the value of explicitly addressing the uncertainty in making decisions, specifically evaluating the effect of model parameters such as the minimum time charter duration and the look-ahead planning horizon. Section 6 provides conclusions and a discussion of future work.

## 2. Problem description and mathematical formulation

In this section, we present a mathematical description of the fleet renewal and deployment problem under uncertainty. As it falls under the broad class of sequential decision making problems, there are numerous mathematical frameworks to tackle the problem, e.g., stochastic programming (Shapiro et al., 2014), adjustable robust optimization (Ben-Tal et al., 2009), and stochastic dynamic programming (Powell, 2011). We adopt a multi-stage stochastic programming framework for describing and modeling the problem, while borrowing some concepts from stochastic dynamic programming to evaluate our policies.

### 2.1. Problem description

Let $\mathcal{K} = \{\text{Owned}, \text{Time Chartered(TC)}, \text{Voyage Chartered(VC)}\}$ be the three vessel types available to the shipper, and let $\mathcal{K}' = \{\text{Owned}, \text{Time Chartered(TC)}\}$. Let $\mathcal{VC} = \{1, \ldots, VC\}$ be the set of available vessel classes, indexed by $vc$, and $\mathcal{F}_{vc} = \{1, \ldots, F_{vc}\}$ be the set of fare classes, indexed by $f$, relevant only for time charter vessels in vessel class $vc$. Vessel classes are distinguished by age, bulk capacity, service speed, and charter rates. We assume that all vessels in vessel class $vc$ have capacity $Q_{vc}$. Fare classes further distinguish vessels by setting an upper bound $M_{vc,f}$ on the number of vessels in vessel class $vc \in \mathcal{VC}$ that can be time chartered at fare $f \in \mathcal{F}_{vc}$. This concept is introduced and utilized in Pantuso et al. (2014b) and Pantuso et al. (2016) to model linearly the fact that as the demand for chartering a certain type of vessel increases the time charter cost of the vessel also increases. Therefore, when all vessels available at a certain fare are time chartered, the next vessel to be time chartered would be chartered at a more expensive fare. We assume that the planning horizon is defined over a set of periods $\mathcal{T} = \{1, \ldots, T\}$, indexed by $t$, where $T$ is the final period of the planning horizon. One could argue that the true problem has an infinite horizon; however, in practice and for well justified business reasons, one is only concerned with a finite horizon.

Let $\mathcal{L} = \{1, \ldots, L\}$ be the set of loading ports, indexed by $l$, $\mathcal{D} = \{1, \ldots, D\}$ be the set of discharging ports, indexed by $d$, and $\mathcal{J} = \mathcal{L} \cup \mathcal{D}$ be the set of all ports. We assume that vessels travel along paths (or routes). Let $\mathcal{P}$ be the set of all possible paths, indexed by $p$, where a path is given by a predefined sequence $\{l_1, l_2, \ldots, l_m, d_1, d_2, \ldots, d_n, l_1\}$ of port calls and corresponding load/discharge amounts $\{\overline{Q}_{vc,p,l_1}, \ldots, \overline{Q}_{vc,p,l_m}, \overline{Q}_{vc,p,d_1}, \ldots, \overline{Q}_{vc,p,d_n}, 0\}$ such that $\sum_{i=1}^{m} \overline{Q}_{vc,p,l_i} = \sum_{i=1}^{n} \overline{Q}_{vc,p,d_i} = Q_{vc}$. That is, a vessel in vessel class $vc$ servicing path $p$ loads or discharges the amount $\overline{Q}_{vc,p,j} \in (0, Q_{vc}]$ at port $j$. The duration of each path is given by $D_{p,vc,t}$ for $p \in \mathcal{P}$, $vc \in \mathcal{VC}$, and $t \in \mathcal{T}$. Note that a path is defined by two attributes, the sequence of port calls and associated loading/discharging quantities, not just by the sequence of port calls alone. Thus, it is possible for two paths to include the same port sequence, but involve different loading/discharging quantities at these ports. In our setting, paths are restricted to a sequence of one or more consecutive loading port calls $\{l_1, \ldots, l_m\}$ followed by a sequence of one or more consecutive discharging port calls $\{d_1, \ldots, d_n\}$. This restriction is due to the fact that this model is meant to straddle strategic and tactical planning and, therefore, purposefully sacrifices certain operational details in order to balance fine-grained details with computational tractability. Finally, note that complicated paths in which a single port (except for the initial loading port $l_1$) is visited multiple times are not considered.

Let $\overline{T}$ denote the duration in days of each time period. A vessel in class $vc$ can make a maximum number of $\left\lfloor \frac{\overline{T}}{D_{p,vc,t}} \right\rfloor$ trips on path $p$ to satisfy customer demand. In some circumstances, the shipping company may choose to keep some inventory at the discharging ports as long as the storage capacities are respected. We assume that the minimum and maximum inventory that can be stored at discharging port $d$ at the end of time period $t$ are 0 and $\overline{S}_{d,t}$, respectively. When a period represents many months, little inventory can be stored from one period to another relative to the total amount consumed in a period. However, for problems with shorter time horizons, inventory may be an important feature. Hence, for generality, we include it in our model. Finally, we assume that loading ports always have an incentive and the capability to produce enough product to meet demand; thus, we do not track production or inventory at loading ports.

There are three stochastic parameters in this model: The demand $\tilde{\Delta}_{d,t}$ at each discharging port $d$ in each time period $t$; the time charter cost $\widetilde{C}^{\text{TC}}_{l,vc,f,t_1,t_2}$ (which includes such costs as crew wages, insurance, and maintenance) for a vessel in vessel class $vc$ and fare class $f$ based in loading port $l$ from the end of time period $t_1$ up to and including the end of time period $t_2$ ($t_2 > t_1$); the voyage charter rate $\widetilde{C}^{\text{VC}}_{p,vc,t}$ for a vessel in class $vc$ serving path $p$ in time period $t$. We assume that all three parameters evolve according to a discrete-time stochastic process. Note that the time charter rate $\widetilde{C}^{\text{TC}}_{l,vc,f,t_1,t_2}$ depends on the loading port $l$ because rates often vary depending on the region of the world in which a vessel is operating.

Additional cost parameters include: $C^{\text{V+O}}_{p,vc,k,t}$, the voyage and operating (V + O) cost of deploying a type $k \in \mathcal{K}'$ vessel in vessel class $vc$ on path $p$ during time period $t$; $C^{\text{Repo}}_{l,l',vc,k,t}$, the repositioning (Repo) cost associated with reassigning company owned or time chartered vessel of class $vc$ from loading port $l$ to loading port $l'$ at the beginning of time period $t$. To be precise, voyage costs include fuel costs, port fees, and canal transit fees, while operating costs include provisions, supplies, lubrication oil, water, and overheads. Note that these costs could also be modeled as stochastic parameters. However, they have less impact on the key decisions being made.

The timing of events and decisions is illustrated in Fig. 1. At the beginning of each time period $t$, exogeneous information becomes available. Specifically, the true market condition is revealed as well as all random parameters indexed by $t$. Then, time charter vessels that were chartered in a previous period are repositioned among loading ports. After these decisions are made, voyage charter vessels may be acquired for a specific one-time voyage servicing a predefined path, and all vessels are deployed to satisfy demand for that period. Time chartering decisions, which can be viewed as strategic decisions, are made at the end of each time period. This is because time chartered vessels are available for use in time periods $t+1, \ldots, t+\tau$, where the time charter duration $\tau$ needs to be determined. Such long-term decisions are made before any random parameters in the future (those indexed by $t'' > t$) are revealed. Finally, vessels time chartered in a previous time period up to time period $t$ exit the fleet. Our main goal in each time period is to determine the number of vessels in each vessel class to time charter and their respective time charter durations.

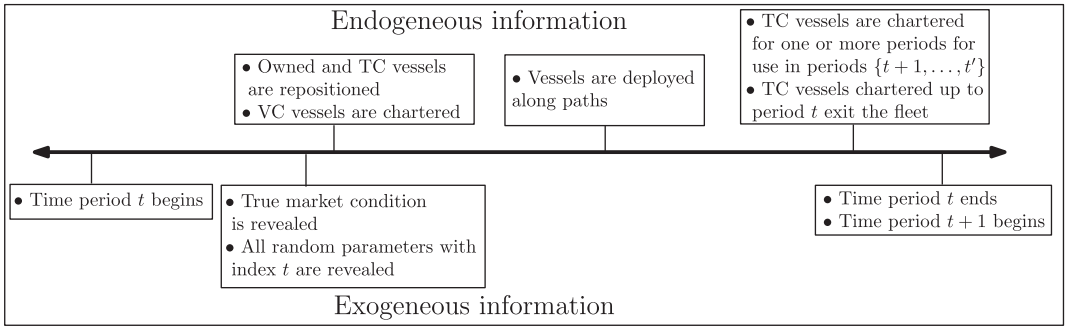


**Fig. 1.** Timing of events and decisions. TC = time charter; VC = voyage charter.

For ease of reference, our main assumptions throughout are: (1) The set $\mathcal{P}$ of paths is given as input; column generation is not assumed. (2) It is not possible (there is no incentive) to charter out vessels to other companies during the planning horizon. However, it would be straightforward to include this feature in the model. (3) Travel costs do not change throughout the planning horizon. In reality, bunker costs fluctuate with global crude prices and other economic factors. However, since fuel costs have a proportional impact on voyage costs, we believe that capturing the relative cost difference between time and voyage charter costs is sufficient. (4) Time chartered vessels may only be repositioned between loading ports once per time period. (5) Chartering contracts are simple and do not include additional options to extend an existing time charter beyond its initial duration. (6) Vessel travel times are deterministic. (7) Loading ports always have an incentive and the ability (collectively) to produce enough product to meet demand; individual loading ports may have limited production capacity.

### 2.2. A multi-stage stochastic programming formulation

Our problem naturally fits the mold of a sequential decision problem under uncertainty, which evolves as follows; see Georghiou et al. (2011). A decision maker first observes an uncertain parameter or vector $\tilde{\xi}_1$ and then takes a decision $\mathbf{x}_1 = X_1(\tilde{\xi}_1)$, i.e., the decision is a function of the realized parameters. After which, a second uncertain parameter $\tilde{\xi}_2$ is revealed, giving the decision maker an opportunity to take a second decision $\mathbf{x}_2 = X_2(\tilde{\xi}_1, \tilde{\xi}_2)$. This sequence of alternating observations and decisions unfolds over $T$ stages, where in each stage $t \in \mathcal{T}$, the decision maker observes an uncertain parameter $\tilde{\xi}_t$ and selects a decision $\mathbf{x}_t = X_t(\tilde{\xi}_{[t]})$, a decision which depends on the whole history of past observations $\tilde{\xi}_{[t]} = (\tilde{\xi}_1, \ldots, \tilde{\xi}_t)$, but not on any future observations $\tilde{\xi}_{t+1}, \ldots, \tilde{\xi}_T$. Here, $X_t(\tilde{\xi}_{[t]})$ is referred to as a decision function, decision rule, decision policy, control law, control policy, or simply a "policy" (the term we will use) depending on the research community where the technique is employed. Our ultimate goal is to provide an explicit functional form of $X_t(\tilde{\xi}_{[t]})$, which may require solving a non-trivial optimization problem itself, that tells a decision maker what decision to implement in time period $t$ as a function of all random parameters that have been observed up to and including time period $t$.

Following the notation given in Chapter 3 of Shapiro et al. (2014), we now present a multi-stage mixed-integer linear stochastic programming formulation of our problem, which will take the following form:

$$\min \quad C_0(\mathbf{x}_0) + \mathbb{E}\left[\sum_{t\in\mathcal{T}} \gamma^t C_t(\mathbf{x}_t, \tilde{\xi}_t)\right] \tag{1a}$$

$$\text{s.t.} \quad X_t(\tilde{\xi}_{[t]}) \in \mathcal{X}_t(X_{t-1}(\tilde{\xi}_{[t-1]}), \tilde{\xi}_t) \quad \forall t \in \mathcal{T} \tag{1b}$$

$$\mathbf{x}_t = X_t(\tilde{\xi}_{[t]}) \quad \forall t \in \mathcal{T} \tag{1c}$$

$$\mathbf{x}_0 \in \mathcal{X}_0. \tag{1d}$$

This formulation assumes that, in each stage $t \in \mathcal{T}$, there is a linear cost function $C_t$ that depends on the decision $\mathbf{x}_t = X_t(\tilde{\xi}_{[t]})$ and the observed random vector $\tilde{\xi}_t$, as well as a feasible region $\mathcal{X}_t$ that depends on the previous decision $X_{t-1}(\tilde{\xi}_{[t-1]})$ made in stage $t-1$ and $\tilde{\xi}_t$. The parameter $\gamma \in (0, 1]$ is a discount factor to account for the time value of money. Here, $C_0$ and $\mathcal{X}_0$ denote the cost function and feasible region, both deterministic, for an initial decision that is made independent of any random parameters. It is important to note that a random variable $\tilde{\xi}_t$ is only random for all $t' < t$. At time $t$, $\tilde{\xi}_t$ is realized and is therefore no longer random.

Before proceeding, it is important to explain why we have chosen to adopt a risk-neutral stochastic programming framework over some other popular optimization under uncertainty frameworks, e.g., robust optimization and risk-averse stochastic programming. Robust optimization, which was applied to fleet sizing in Alvarez et al. (2011), takes a

distribution-free approach to random events, and instead relies on uncertainty sets to immunize decisions against the worst-case outcome in the uncertainty set. As discussed in Ben-Tal et al. (2009), such an approach is well suited for situations when the worst case outcomes have severe or catastrophic consequences, such as causing an individual or company to go bankrupt. Because our problem involves decisions made rather frequently over time, e.g., every three to six months, with recourse opportunities to avoid catastrophe, a stochastic programming approach that uses distributional information seems justified. In addition, fleet planners currently rely on scenarios, some of which are deemed more likely than others, and thus are more willing to accept this approach. One could argue that a risk-averse objective function, e.g., using a popular conditional value-at-risk metric (Rockafellar and Uryasev, 2000), is also warranted. We believe that a risk-averse approach could be useful if chartering decisions were made less frequently, and thus the consequences of each decision were more profound.

Our goal in the remainder of this section is to explicitly define each of the components in (1). We begin with the decision variables, all of which are denoted with lower case Roman characters. Let $x^{\mathrm{TC}}_{l,vc,f,t_1,t_2}$ denote the integer number of time chartered vessels, initially chartered for and assigned to loading port $l$, in vessel class $vc$ and fare class $f$ that are chartered *at the end* of time period $t_1$ and that serve in the fleet in time periods $t_1+1,\ldots,t_2$. Let $y^{\mathrm{TC,Exit}}_{l,vc,t}$ denote the integer number of time chartered vessels in vessel class $vc$ exiting the fleet *at the end* of time period $t$ from loading port $l$. Let $y^{\mathrm{Repo}}_{l,l',vc,k,t}$ denote the integer number of type $k\in\mathcal{K}'$ vessels in vessel class $vc$ repositioned from loading port $l$ to loading port $l'$ *at the beginning* of time period $t$. Let $y_{l,vc,k,t}$ be the integer number of type $k\in\mathcal{K}'$ vessels in vessel class $vc$ assigned to loading port $l$ for the duration of time period $t$ after repositioning decisions have been made. Let $z_{p,vc,k,t}$ be the (possibly fractional) number of trips made on path $p$ using type $k\in\mathcal{K}$ vessels of class $vc$ during time period $t$. Let $s_{d,t}$ denote the inventory level at discharging port $d$ *at the end of* time period $t$. Collectively, we will write all decision variables at time $t$ as a single vector $\mathbf{x}_t=(\mathbf{x}^{\mathrm{TC}}_t,\mathbf{y}^{\mathrm{TC,Exit}}_t,\mathbf{y}^{\mathrm{Repo}}_t,\mathbf{y}_t,\mathbf{z}_t,\mathbf{s}_t)$ in agreement with the notation in (1). To be clear, a decision vector indexed by $t$ includes all corresponding decision variables in time period $t$, e.g., $\mathbf{x}^{\mathrm{TC}}_t=\{x^{\mathrm{TC}}_{l,vc,f,t,t'}\}_{l,vc,f,t'>t}$.

It is important to note that all of the decision variables introduced above are actually functions of the random vector $\tilde{\boldsymbol{\xi}}_{[t]}$, where, in our problem, $\tilde{\boldsymbol{\xi}}_t=(\tilde{\boldsymbol{\Delta}}_t,\tilde{\mathbf{C}}^{\mathrm{TC}}_t,\tilde{\mathbf{C}}^{\mathrm{VC}}_t)$ denotes (the vector of) all random variables that become known at the beginning of time period $t$ before any decisions in period $t$ are made. However, to simplify notation and to make the formulation more consistent with what would appear in a deterministic setting, we use decision variables $\mathbf{x}_t$ and link these variables to their functional form via the constraints $\mathbf{x}_t=X_t(\tilde{\boldsymbol{\xi}}_{[t]})$.

The cost function in each time period $t\in\mathcal{T}$ is given by

$$C_t(\mathbf{x}_t,\tilde{\boldsymbol{\xi}}_t):=\sum_{l,vc,f,t'>t}\widetilde{C}^{\mathrm{TC}}_{l,vc,f,t,t'}x^{\mathrm{TC}}_{l,vc,f,t,t'}+\sum_{p,vc}\widetilde{C}^{\mathrm{VC}}_{p,vc,t}z_{p,vc,\mathrm{VC},t}+\sum_{l,l',vc,k\in\mathcal{K}'}C^{\mathrm{Repo}}_{l,l',vc,k,t}y^{\mathrm{Repo}}_{l,l',vc,k,t}+\sum_{p,vc,k\in\mathcal{K}'}C^{\mathrm{V+O}}_{p,vc,k,t}z_{p,vc,k,t},\tag{2}$$

where, henceforth, if the set over which a sum occurs is omitted, then all elements in the set are assumed to be included in the summation. It includes the cost of time chartering vessels, the cost of voyage chartering vessels to satisfy demand that cannot be met with the time chartered vessel fleet, the cost of repositioning company owned and time chartered vessels, and the variable and operational cost of deploying the time chartered vessels. The cost function $C_0$, associated with an initial decision made prior to any random parameters being revealed, only includes the cost of time chartering decisions and is given by

$$C_0(\mathbf{x}_0):=C_0(\mathbf{x}^{\mathrm{TC}}_0)=\sum_{l,vc,f,t'>0}C^{\mathrm{TC}}_{l,vc,f,0,t'}x^{\mathrm{TC}}_{l,vc,f,0,t'}.\tag{3}$$

Because we consider a finite time horizon, a sunset or salvage value is necessary to value the vessels that have been time chartered beyond the length of the planning horizon. The sunset value of time chartered vessels remaining at the end of the planning horizon is given by the reward function

$$R_{T+1}(\mathbf{x}^{\mathrm{TC}}_0,\mathbf{x}^{\mathrm{TC}}_1,\ldots,\mathbf{x}^{\mathrm{TC}}_T,\tilde{\mathbf{C}}^{\mathrm{TC}}_{T+1})=\sum_{l,vc,f}\sum_{t_1<T}\sum_{t_2>T}\widetilde{C}^{\mathrm{TC}}_{l,vc,f,T+1,t_2}x^{\mathrm{TC}}_{l,vc,f,t_1,t_2}.\tag{4}$$

In words, the actual sunset value of a vessel time chartered in time period $t_1$ (thus beginning service in time period $t_1+1$) until the end of time period $t_2>T$ is the value for a vessel in vessel class $vc$ and fare class $f$ beginning in time period $T+1$ up to and including time period $t_2$. Note that the time chartering coefficients $\widetilde{C}^{\mathrm{TC}}_{l,vc,f,T+1,t_2}$ only become known in time period $T+1$. With this addition, we modify the objective function (1a) to include the discounted reward from all time chartered vessels remaining in the fleet at the end of the $T$-period planning horizon:

$$C_0(\mathbf{x}_0)+\mathbb{E}\left[\sum_{t\in\mathcal{T}}\gamma^tC_t(\mathbf{x}_t,\tilde{\boldsymbol{\xi}}_t)-\gamma^{T+1}R_{T+1}(\mathbf{x}^{\mathrm{TC}}_0,\mathbf{x}^{\mathrm{TC}}_1,\ldots,\mathbf{x}^{\mathrm{TC}}_T,\tilde{\mathbf{C}}^{\mathrm{TC}}_{T+1})\right].\tag{5}$$

The feasible region (also called the set of implementable policies) $\mathcal{X}_t$ at time period $t$ is

$$\mathcal{X}_t(X_{[t-1]}(\tilde{\boldsymbol{\xi}}_{[t-1]}), \tilde{\boldsymbol{\xi}}_t) = \mathcal{X}_t(\mathbf{x}_{[t-1]}, \tilde{\boldsymbol{\xi}}_t) = \tag{6a}$$

$$\Big\{\mathbf{x}_t = (\mathbf{x}_t^{\mathrm{TC}}, \mathbf{y}_t^{\mathrm{TC,Exit}}, \mathbf{y}_t^{\mathrm{Repo}}, \mathbf{y}_t, \mathbf{z}_t, \mathbf{s}_t) : \tag{6b}$$

$$s_{d,t-1} + \sum_{p\in\mathcal{P}_d}\sum_{vc\in\mathcal{VC}}\sum_{k\in\mathcal{K}} \overline{Q}_{vc,p,d} z_{p,vc,k,t} = \tilde{\Delta}_{d,t} + s_{d,t} \quad \forall d \in \mathcal{D}, t \in \mathcal{T} \tag{6c}$$

$$\sum_{p\in\mathcal{P}_l}\sum_{vc\in\mathcal{VC}}\sum_{k\in\mathcal{K}} \overline{Q}_{vc,p,l} z_{p,vc,k,t} \leqslant P_{l,t} \quad \forall l \in \mathcal{L}, t \in \mathcal{T} \tag{6d}$$

$$y_{l,vc,k,t-1} + \sum_{l'\in\mathcal{L}:l'\neq l} y^{\mathrm{Repo}}_{l',l,vc,k,t} + \sum_{f}\sum_{t'\geqslant t} x^{\mathrm{TC}}_{l,vc,f,t-1,t'}$$
$$= y_{l,vc,k,t} + \sum_{l'\in\mathcal{L}:l'\neq l} y^{\mathrm{Repo}}_{l,l',vc,k,t} + y^{\mathrm{TC,Exit}}_{l,vc,t-1} \quad \forall l \in \mathcal{L}, vc \in \mathcal{VC}, t \in \mathcal{T}, k = \mathrm{TC} \tag{6e}$$

$$y_{l,vc,k,t-1} + \sum_{l'\in\mathcal{L}:l'\neq l} y^{\mathrm{Repo}}_{l',l,vc,k,t}$$
$$= y_{l,vc,k,t} + \sum_{l'\in\mathcal{L}:l'\neq l} y^{\mathrm{Repo}}_{l,l',vc,k,t} \quad \forall l \in \mathcal{L}, vc \in \mathcal{VC}, t \in \mathcal{T}, k = \mathrm{Owned} \tag{6f}$$

$$\sum_{l} y^{\mathrm{TC,Exit}}_{l,vc,t} = \sum_{l}\sum_{f}\sum_{t'<t} x^{\mathrm{TC}}_{l,vc,f,t',t} \quad \forall vc \in \mathcal{VC}, t \in \mathcal{T} \tag{6g}$$

$$\sum_{l}\sum_{t_2>t} x^{\mathrm{TC}}_{l,vc,f,t,t_2} \leqslant M_{vc,f} - \sum_{l}\sum_{t_1<t}\sum_{t_2>t} x^{\mathrm{TC}}_{l,vc,f,t_1,t_2} \quad \forall vc \in \mathcal{VC}, f \in \mathcal{F}_{vc}, t \in \mathcal{T} \tag{6h}$$

$$z_{p,vc,k,t} \leqslant \left\lfloor \frac{\overline{T}}{D_{p,vc,t}} \right\rfloor y_{l,vc,k,t} \quad \forall l \in \mathcal{L}, p \in \mathcal{P}_l^{\mathrm{Origin}}, vc \in \mathcal{VC}, t \in \mathcal{T}, k \in \mathcal{K}' \tag{6i}$$

$$\sum_{p\in\mathcal{P}_l^{\mathrm{Origin}}} D_{p,vc,t} z_{p,vc,k,t} \leqslant \overline{T} y_{l,vc,k,t} \quad \forall l \in \mathcal{L}, vc \in \mathcal{VC}, t \in \mathcal{T}, k \in \mathcal{K}' \tag{6j}$$

$$\sum_{p'\in\mathcal{P}_l^{\mathrm{Origin}}} \left\lfloor \frac{D_{p',vc,t}}{D_{p,vc,t}} \right\rfloor z_{p,vc,k,t} \leqslant \left\lfloor \frac{\overline{T}}{D_{p,vc,t}} \right\rfloor y_{l,vc,k,t} \quad \forall l \in \mathcal{L}, p \in \mathcal{P}_l^{\mathrm{Origin}}, t \in \mathcal{T}, vc \in \mathcal{VC}, k \in \mathcal{K}' \tag{6k}$$

$$0 \leqslant s_{d,t} \leqslant \overline{S}_{d,t} \quad \forall d \in \mathcal{D}, t \in \mathcal{T} \tag{6l}$$

$$x^{\mathrm{TC}}_{l,vc,f,t,t'} \in \mathbb{Z}_+ \quad \forall l \in \mathcal{L}, vc \in \mathcal{VC}, f \in \mathcal{F}_{vc}, t, t' \in \mathcal{T} : t' > t \tag{6m}$$

$$y^{\mathrm{TC,Exit}}_{l,vc,t} \in \mathbb{Z}_+ \quad \forall l \in \mathcal{L}, vc \in \mathcal{VC}, t \in \mathcal{T} \tag{6n}$$

$$y^{\mathrm{Repo}}_{l,l',vc,k,t} \in \mathbb{Z}_+ \quad \forall (l,l') \in \mathcal{L}\times\mathcal{L}, vc \in \mathcal{VC}, t \in \mathcal{T}, k \in \mathcal{K}' \tag{6o}$$

$$y_{l,vc,k,t} \in \mathbb{Z}_+ \quad \forall l \in \mathcal{L}, vc \in \mathcal{VC}, t \in \mathcal{T}, k \in \mathcal{K}' \tag{6p}$$

$$z_{p,vc,k,t} \geqslant 0 \quad \forall p \in \mathcal{P}, vc \in \mathcal{VC}, t \in \mathcal{T}, k \in \mathcal{K}\Big\}. \tag{6q}$$

Note that the feasible set $\mathcal{X}_t$ in (6) is written as a function of the entire decision history $\mathbf{x}_{[t-1]}$ and not simply as a function of $\mathbf{x}_{t-1}$ as shown in (1b). This is because constraints (6e) and (6f) require information from decisions made before period $t-1$. After introducing auxiliary decision variables to track prior time chartering decisions, we could easily modify the feasible set $\mathcal{X}_t$ to be a function only of the previous decision vector $\mathbf{x}_{t-1}$.

Constraints (6c) keep track of the inventory at discharging ports and ensure that demand is satisfied. The left hand side of (6c) includes existing inventory at port $d$ plus the total amount of product discharged by time chartered vessels and voyage chartered vessels. Constraints (6d) limit the amount of product that can be loaded from each loading port $l$ in each time period $t$ to the production limit $P_{l,t}$. Time chartered vessel balance constraints (6e) ensure that, for each vessel class $vc \in \mathcal{VC}$ and each loading port $l \in \mathcal{L}$, the number of time chartered vessels available in the beginning of time period $t$, which can be deployed in period $t$, equals the number of existing time chartered vessels, plus the number of new time chartered vessels entering the fleet initially assigned to loading port $l$, plus the number of time chartered vessels repositioned from another loading port $l'$ to $l$, minus the number of time chartered vessels exiting the fleet, minus the number of time chartered vessels repositioned from $l$ to another loading port $l'$. Constraints (6g) ensure that the correct number of time chartered vessels in vessel class $vc$ exit the fleet in time period $t$. Note that because time chartered vessels can be repositioned from period to period, constraints (6g) sum over all loading ports rather than track the number of vessels exiting the fleet from each individual loading port.

Constraints (6h) ensure that the number of time chartered vessels in vessel class $vc$ and fare class $f$ in period $t$ does not exceed the number $M_{vc,f}$ of vessels available at fare $f$. The left hand side of (6h) is the number of vessels of class $vc$ and fare class $f$ that are time chartered at the end of time period $t$ to join the fleet at the beginning of time period $t+1$. The right hand side is the number of vessels of class $vc$ that are available at fare $f$ minus the number of vessels of class $vc$ time chartered at fare $f$ prior to period $t$ and that are still in the fleet until the end of period $t$. Accordingly constraints (6h) impose that the number of vessels in vessel class $vc$ and fare class $f$ that are in the fleet during time period $t$ should be less than the fare capacity $M_{vc,f}$.

Constraints (6i)–(6k) define the relationship between the deployment decisions and time charter decisions. Constraints (6i) give the upper bound on the number of trips serving each path $p$ for each vessel class $vc$. This is simply the number of vessels assigned to a loading port $l$ multiplied by the number of times path $p$ can be serviced, within $\overline{T}$ days, by a single vessel. Constraints (6j) aggregate constraints (6i) across all trips that originate from loading port $l$.

Our modeling of the deployment and how it compares to some other studies in the literature is worth further discussion. In our model, vessels are assigned to a loading port for the entire duration of a time period. Consequently, they can only perform voyages starting and ending at this loading port. On the other hand, at the end of each time period, we may decide to relocate a vessel from one loading port to another. As mentioned before we assume that vessels may be relocated only once in a period. We do not explicitly account for the travel time incurred repositioning vessels between loading ports. The reason for this is that, with this coarse representation of deployment, it is not clear how much travel time will actually be incurred. For example, suppose a vessel is repositioned between two loading ports at the beginning of time period $t$. Our model assumes that the vessel must complete roundtrips, i.e., each vessel's starting and ending location in each period is at the same loading port. In reality, at the end of the period, a vessel could make a one-way voyage to a demand port and then a one-way voyage to a *different* loading port, a voyage that could potentially eliminate any repositioning time between loading ports. Bakkehaug et al. (2014) and Pantuso et al. (2016) assume that trades are single-origin/single-destination routes. Pantuso et al. (2016) describe a loop as a ship route that starts and ends in the same geographic area after servicing, in a given order, a number of trades. Loops of cardinality greater than two represent Hamiltonian cycles. Bakkehaug et al. (2014) only consider loops of cardinality one. Pantuso et al. (2016) consider loops of shortest distance and for the most part of cardinality two (although in one subsection loops of cardinality up to five are considered) in their computational study. They do not take into account the sailing between loops. Their justification of this assumption is similar to ours. They also assume that fleet renewal plans are made at the end of any period.

Constraints (6i) and (6j) treat the available time for each vessel as an aggregated resource. As a consequence, without constraints (6k), the number of trips that can be performed by each vessel class is overestimated as a single voyage can be split across multiple vessels. In such cases, the total cost is underestimated as the model assumes that a single voyage takes place, when in reality multiple voyages were required. Constraints (6k) eliminate such solutions by placing additional bounds on the number of trips that can be performed by a vessel class on path $p$ that originate from loading port $l$. In constraints (6i)–(6k), we assume that the maximum number of voyages that can be performed by a vessel is integer and therefore vessels may only start a voyage in period $t$ if they can complete the voyage within the same time period. One might argue that this leads to inefficient fleet utilization. However, there are two reasons for this modeling choice. First, by imposing these bounds, we make sure that the vessels are available for repositioning at their origin port at the beginning of each period. Second, this approach may leave some slack time in a vessel's schedule to deal with operational details not accounted for in the model, such as stochasticity of travel times, layovers at discharge ports, and time spent in maintenance.

Finally, constraints (6l)–(6q) are variable bound constraints.

## 3. Solution methods and look-ahead policies

Model (1a)–(1d) in our setting is a multi-stage stochastic integer program with mixed-integer recourse. As such, it is extremely difficult to solve to provable optimality. Consequently, we turn to approximation strategies that provide good policies in practice since we are most interested in making judicious time chartering decisions in each time period. Powell (2011) describes four broad categories of policies for stochastic optimization: myopic policies, look-ahead policies, policy function approximations, and value function approximations. Myopic policies are the most elementary as they do not explicitly use forecasted information, but instead rely on tunable parameters to yield acceptable outcomes. Policy function approximations return a decision given the current state of the system without using any form of embedded optimization or forecasted information. Value function approximations attempt to approximate the value of being in a future state as a result of a decision made in the present and typically require a fair amount of on- or off-training, a computational component that is foreign to most business analysts. In this section, we describe our approach using a stochastic look-ahead model. Although Powell (2014) claims that this is the most complex type of look-ahead function, it is a natural progression from the ad hoc scenario-based approach that practitioners currently use in this domain. Indeed, since practitioners are already accustomed to constructing scenarios and applying optimization, this approach is likely to expedite adoption for commercial use.

Look-ahead policies rely on a rolling horizon procedure, also called a receding horizon procedure or model predictive control, an idea that dates back to the control literature of the 1960s, if not earlier (García et al., 1989). In each time period $t$, we solve an approximation of Model (1a)–(1d) over a limited time horizon to determine our here-and-now decision (i.e., the number of vessels to time charter and the corresponding charter duration). To accomplish this, we follow a standard approach in computational stochastic optimization and discretize the underlying random process. Specifically, we build a scenario tree (described below) based on a number of sample paths and construct the so-called deterministic equivalent of the stochastic program, which in our setting can be solved using existing optimization technology.

To construct our look-ahead model at time $t$, we assume that the stochastic parameters $\tilde{\xi}_t$ evolve according to a discrete-time stochastic process with finite probability space. This process is modeled as a scenario tree with $H+1$ stages (i.e., an $H$-period look-ahead where $H \leqslant T$) and a set $\mathcal{N} = \{0, \ldots, N\}$ of nodes. Analogous to Model (1a)–(1d), all here-and-now

decisions are made in stage 0, whereas wait-and-see decisions are made in stages $1,\ldots,H$. We refer to the root node as node 0, a node at stage $H$ as a leaf node, and the set of all leaf nodes as $\mathcal{N}^L$. A node $n$ at stage $h(n)$ of the scenario tree gives the information state of the system that can be distinguished by information available up to stage $h(n)$ and represents a joint realization vector $(\tilde{\xi}_{t+1},\ldots,\tilde{\xi}_{t+h(n)})$ of the random variables. Let $t(n)$ denote the time period relative to Model (1a)–(1d) associated with node $n$. To be clear, $t(n)\in\{0,1,\ldots,T\}$, while $h(n)\in\{0,1,\ldots,H\}$ where $H\leqslant T$ for each node $n\in\mathcal{N}$. Let $\pi_n$ denote the probability associated with the state represented by node $n\in\mathcal{N}$ and $a(n)$ the unique parent (ancestor) associated with node $n\in\mathcal{N}$. We define $\mathcal{R}(n)=\{a(n),a(a(n)),\ldots,0\}$ as the set of ancestor nodes on the path from the root node 0 to node $n$. Therefore, each path $\mathcal{R}(n)$ for $n\in\mathcal{N}^L$ corresponds to a complete scenario of realizations $(\tilde{\xi}_{t+1},\ldots,\tilde{\xi}_{t+H})$ for the random parameter $\tilde{\xi}$. Fig. 2 illustrates these concepts with a scenario tree having two branches at every node. The number of branches per node is an important parameter of the scenario tree, as it determines the portfolio of scenarios examined by the model, and is explored in Section 5.

With an abuse of notation, we re-define the decision variables and parameters (deterministic and stochastic alike) in Section 2.2 to include a node index $n$ in lieu of a time index $t$. In particular, all decision variables and parameters containing the index $t$ in the previous section are modified to handle the scenario tree representation. Henceforth, a variable should be understood with a node index $n$. Rather than re-list all decision variables and parameters, we note a few examples. Let $x^{\mathrm{TC}}_{l,vc,f,n,t'}$ denote the integer number of time chartered vessels, at node $n$ of the scenario tree, initially chartered for and assigned to loading port $l$, in vessel class $vc$ and fare class $f$ that are chartered at the end of time period $t(n)$ and are available for service in time periods $t(n)+1,\ldots,t'$. Let $y^{\mathrm{TC,Exit}}_{l,vc,n}$ denote the integer number of time charter vessels in vessel class $vc$ exiting the fleet *at the end* of time period $t(n)$ from loading port $l$, at node $n$ of the scenario tree. Let $y^{\mathrm{Repo}}_{l,l',vc,k,n}$ denote the integer number of type $k\in\mathcal{K}'$ vessels in vessel class $vc$ repositioned from loading port $l$ to loading port $l'$ *at the beginning* of time period $t(n)$, at node $n$ of the scenario tree. Let $y_{l,vc,k,n}$ be the number of type $k\in\mathcal{K}'$ vessels in vessel class $vc$ assigned to loading port $l$ in time period $t(n)$ after repositioning decisions have been made, at node $n$ of the scenario tree. Let $z_{p,vc,k,n}$ be the (possibly fractional) number of trips made on path $p$ using type $k\in\mathcal{K}$ vessels of class $vc$ during time period $t(n)$, at node $n$ of the scenario tree. The demand $\tilde{\Delta}_{d,t}$ at each discharging port $d$ in each time period $t$ is now written as $\Delta_{d,n}$. Note that the tilde has been removed since $\Delta_{d,n}$ is a known value in the look-ahead model. Similarly, the time charter cost $\tilde{C}^{\mathrm{TC}}_{l,vc,f,t_1,t_2}$ is now written as $C^{\mathrm{TC}}_{l,vc,f,n,t_2}$ for a vessel in vessel class $vc$ and fare class $f$ based in loading port $l$ from the beginning of time period $t(n)+1$ until the end of time period $t_2$ ($t_2\geqslant t(n)$).

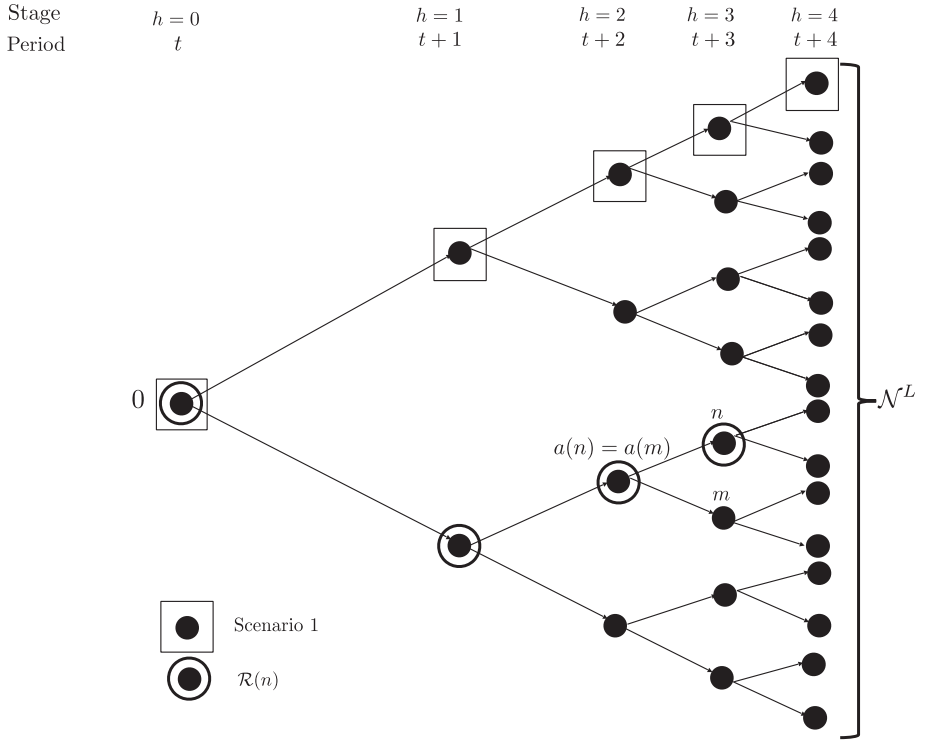


**Fig. 2.** Scenario tree structure.

The purpose of solving the look-ahead model is to make judicious time chartering decisions as shown in the last step of Fig. 1. Consequently, our look-ahead model is solved in each time period $t \in \mathcal{T}$ and is always solved with a look-ahead horizon $H$ (an integer that is held constant), even as we reach the end of the planning horizon (i.e., as $t$ approaches $T$). We assume that we can sample random parameters $\tilde{\xi}_t$ for $t > T$. Rather than truncate the look-ahead horizon, we keep it fixed because this is what is done in practice; the actual business problem does not terminate in time period $T$. This is also common in the control literature where one aims to control a process for many periods. After a chartering decision is made in time period $t$, the next iteration of the rolling horizon procedure occurs. This process mimics the timing of events and decisions illustrated in Fig. 1. In Section 5, we explain how this approach can easily be evaluated in a simulation framework.

To capture existing information from decisions made in a previous time period, we need to introduce the following parameters for the root node of the scenario tree: $\hat{s}_{d,0}$, the ending inventory at demand port $d$ in time period $t$ that is available at the start of stage 1 (period $t+1$); $\hat{x}^{\mathrm{TC}}_{l,vc,f,t_1,t_2}$, the number of time charter vessels acquired in time period $t_1$ (before the current time period $t$) until the end of time period $t_2 > t$ and still in the fleet; $\hat{y}^{\mathrm{TC,Exit}}_{l,vc,0}$, the integer number of time chartered vessels that exited the fleet at the end of time period $t$; $\hat{y}_{l,vc,k,0}$, the integer number of type $k \in \mathcal{K}'$ vessels available at port $l$ at the end of time period $t$, which are available for use in stage 1 (period $t+1$). Note that we need to track both $\hat{x}^{\mathrm{TC}}_{l,vc,f,t_1,t_2}$ and $\hat{y}_{l,vc,k,0}$ since the former tracks the age (or remaining time in the fleet) whereas the latter tracks the starting vessel location in each time period, but not the age.

The cost function at each non-root node $n \in \mathcal{N} \setminus \{0\}$ is just a modification of (2), and is given by

$$C_n(\mathbf{x}_n, \xi_n) := \sum_{l,vc,f,t' > t(n)} C^{\mathrm{TC}}_{l,vc,f,n,t'} x^{\mathrm{TC}}_{l,vc,f,n,t'} + \sum_{p,vc} C^{\mathrm{VC}}_{p,vc,n} z_{p,vc,\mathrm{VC},n} + \sum_{l,l',vc,k \in \mathcal{K}'} C^{\mathrm{Repo}}_{l,l',vc,k,n} y^{\mathrm{Repo}}_{l,l',vc,k,n} + \sum_{p,vc,k \in \mathcal{K}'} C^{\mathrm{V+O}}_{p,vc,k} z_{p,vc,k,n}. \tag{7}$$

The cost function at the root node $n = 0$ is simpler, since no deployment decisions are made (in fact, they have already been made) in the corresponding period $t(0)$, and is given by

$$C_0(\mathbf{x}_0) := C_0(\mathbf{x}^{\mathrm{TC}}_0) = \sum_{l,vc,f,t' > t(0)} C^{\mathrm{TC}}_{l,vc,f,0,t'} x^{\mathrm{TC}}_{l,vc,f,0,t'}. \tag{8}$$

With these modifications, the look-ahead model that we solve in each time period $t \in \mathcal{T}$ is a simple adaptation of the model presented in Section 2.

$$\min C_0(\mathbf{x}_0) + \sum_{n \in \mathcal{N} \setminus \{0\}} \pi_n \gamma^{t(n)-t} C_n(\mathbf{x}_n, \xi_n) \tag{9a}$$

$$\text{s.t.} \; s_{d,a(n)} + \sum_{p \in \mathcal{P}_d} \sum_{vc \in \mathcal{VC}} \sum_{k \in \mathcal{K}} \overline{Q}_{vc,p,d} z_{p,vc,k,n} = \Delta_{d,n} + s_{d,n} \quad \forall d \in \mathcal{D}, n \in \mathcal{N} \setminus \{0\} \tag{9b}$$

$$\sum_{p \in \mathcal{P}_l} \sum_{vc \in \mathcal{VC}} \sum_{k \in \mathcal{K}} \overline{Q}_{vc,p,l} z_{p,vc,k,n} \leqslant P_{l,t} \quad \forall l \in \mathcal{L}, n \in \mathcal{N} \setminus \{0\} \tag{9c}$$

$$y_{l,vc,k,a(n)} + \sum_{l' \in \mathcal{L}: l' \neq l} y^{\mathrm{Repo}}_{l',l,vc,k,n} + \sum_{f} \sum_{t' > t(n)} x^{\mathrm{TC}}_{l,vc,f,n,t'} = y_{l,vc,k,n} + \sum_{l' \in \mathcal{L}: l' \neq l} y^{\mathrm{Repo}}_{l,l',vc,k,n} + y^{\mathrm{TC,Exit}}_{l,vc,a(n)} \quad \forall l \in \mathcal{L}, vc \in \mathcal{VC}, n \in \mathcal{N} \setminus \{0\} k = \mathrm{TC} \tag{9d}$$

$$y_{l,vc,k,a(n)} + \sum_{l' \in \mathcal{L}: l' \neq l} y^{\mathrm{Repo}}_{l',l,vc,k,n} = y_{l,vc,k,n} + \sum_{l' \in \mathcal{L}: l' \neq l} y^{\mathrm{Repo}}_{l,l',vc,k,n} \quad \forall l \in \mathcal{L}, vc \in \mathcal{VC}, n \in \mathcal{N} \setminus \{0\} k = \mathrm{Owned} \tag{9e}$$

$$\sum_{l \in \mathcal{L}} y^{\mathrm{TC,Exit}}_{l,vc,n} = \sum_{l \in \mathcal{L}} \sum_{f} \left[ \sum_{n' \in \mathcal{R}(n)} x^{\mathrm{TC}}_{l,vc,f,n',t(n)} + \sum_{t' < t(0)} \hat{x}^{\mathrm{TC}}_{l,vc,f,t',t(n)} \right] \quad \forall vc \in \mathcal{VC}, n \in \mathcal{N} \setminus \{0\} \tag{9f}$$

$$\sum_{l \in \mathcal{L}} \sum_{t_2 > t(n)} x^{\mathrm{TC}}_{l,vc,f,n,t_2} \leqslant M_{vc,f} - \sum_{l \in \mathcal{L}} \sum_{t_2 \geqslant t(n)} \left[ \sum_{n' \in \mathcal{R}(n)} x^{\mathrm{TC}}_{l,vc,f,n',t_2} + \sum_{t_1 < t(0)} \hat{x}^{\mathrm{TC}}_{l,vc,f,t_1,t_2} \right] \quad \forall vc \in \mathcal{VC}, f \in \mathcal{F}_{vc}, n \in \mathcal{N} \tag{9g}$$

$$z_{p,vc,k,n} \leqslant \left\lfloor \frac{\overline{T}}{D_{p,vc,t(n)}} \right\rfloor y_{l,vc,k,n} \quad \forall l \in \mathcal{L}, \mathcal{P}^{\mathrm{Origin}}_l, vc \in \mathcal{VC}, n \in \mathcal{N} \setminus \{0\}, k \in \mathcal{K}' \tag{9h}$$

$$\sum_{p \in \mathcal{P}^{\mathrm{Origin}}_l} D_{p,vc,t(n)} z_{p,vc,k,n} \leqslant \overline{T} y_{l,vc,k,n} \quad \forall l \in \mathcal{L}, vc \in \mathcal{VC}, n \in \mathcal{N} \setminus \{0\}, k \in \mathcal{K}' \tag{9i}$$

$$\sum_{p' \in \mathcal{P}^{\mathrm{Origin}}_l} \left\lfloor \frac{D_{p',vc,t(n)}}{D_{p,vc,t(n)}} \right\rfloor z_{p,vc,k,n} \leqslant \left\lfloor \frac{\overline{T}}{D_{p,vc,t(n)}} \right\rfloor y_{l,vc,k,n} \quad \forall l \in \mathcal{L}, p \in \mathcal{P}^{\mathrm{Origin}}_l, vc \in \mathcal{VC}, n \in \mathcal{N} \setminus \{0\} \tag{9j}$$

$$0 \leqslant s_{d,n} \leqslant \overline{S}_{d,t(n)} \quad \forall d \in \mathcal{D}, n \in \mathcal{N} \setminus \{0\} \tag{9k}$$

$$x^{\mathrm{TC}}_{l,vc,f,n,t'} \in \mathbb{Z}_+ \quad \forall l \in \mathcal{L}, vc \in \mathcal{VC}, f \in \mathcal{F}_{vc}, n \in \mathcal{N}, t' > t(n) \tag{9l}$$

$$y^{\mathrm{TC,Exit}}_{l,vc,n} \in \mathbb{Z}_+ \quad \forall l \in \mathcal{L}, vc \in \mathcal{VC}, n \in \mathcal{N} \tag{9m}$$

$$y^{\mathrm{Repo}}_{l,l',vc,k,n} \in \mathbb{Z}_+ \quad \forall (l,l') \in \mathcal{L} \times \mathcal{L}, vc \in \mathcal{VC}, k \in \mathcal{K}', n \in \mathcal{N} \setminus \{0\} \tag{9n}$$

$$y_{l,vc,k,n} \in \mathbb{Z}_+ \quad \forall l \in \mathcal{L}, vc \in \mathcal{VC}, k \in \mathcal{K}', n \in \mathcal{N} \tag{9o}$$

$$z_{p,vc,k,n} \geqslant 0 \quad \forall p \in \mathcal{P}, vc \in \mathcal{VC}, n \in \mathcal{N} \setminus \{0\}, k \in \mathcal{K} \tag{9p}$$

$$s_{d,0} = \hat{s}_{d,0} \quad \forall d \in \mathcal{D} \tag{9q}$$

$$y^{\text{TC,Exit}}_{l,vc,0} = \hat{y}^{\text{TC,Exit}}_{l,vc,0} \quad \forall l \in \mathcal{L}, vc \in \mathcal{VC} \tag{9r}$$

$$y_{l,vc,k,0} = \hat{y}_{l,vc,k,0} \quad \forall l \in \mathcal{L}, vc \in \mathcal{VC}, k \in \mathcal{K}' \tag{9s}$$

On the whole, the feasible region of this model looks, quite intentionally, like that of model (6). Noteworthy differences are: (1) In the look-ahead model (9), there are no random parameters. The scenario tree is a set of sample paths, meaning that all data is deterministic. (2) The look-ahead horizon is $H$, not $T$. (3) The look-ahead model is solved at each time step. (4) This model is solved after all deployment decisions in time period $t$ have been made. (5) The only structural (non-bound) constraints that apply at the root node $n = 0$ are the fare class limit constraints (9g). (6) Non-anticipativity is captured by the fact that constraints (9b) and (9d) are written with respect to the ancestor node $a(n)$. (7) Constraints (9f) and (9g) are similar to constraints (6g) and (6h). (8) Constraints (9q)–(9s) set the initial conditions at the root node to account for decisions made in previous periods.

Below we outline three approaches that use the look-ahead model (9). These are compared computationally in Section 5. It is worth noting that Pantuso et al. (2016) compare the scenario tree solution (Section 3.1) to the expected value solution (Section 3.2) in their computational study. We additionally introduce an ad hoc scenario average solution method (Section 3.3).

### 3.1. Stochastic programming solution using a multi-scenario stochastic forecast

In this approach, we generate a multi-scenario stochastic forecast (i.e., a scenario tree) and solve look-ahead model (9) in each time period in the rolling horizon algorithm. We implement the time chartering decision made at stage 0 and then roll forward. This is the most complicated policy that we explore. In our computational section, we solve the extensive form or deterministic equivalent of model (9) using a commercial mixed-integer linear programming solver. We also evaluate the performance of different scenario trees with varying look-ahead horizons $H$.

### 3.2. Expected value solution using a single-scenario deterministic forecast

One of the simplest look-ahead policies is to generate a single scenario (or single sample path of the underlying random variables) by considering the expected value of the random parameters in all time periods considered in the look-ahead horizon. Specifically, if we are currently in time period $t$, then a point forecast of random parameters over the next $H$ periods is used, i.e., we use the sample $\mathbb{E}[\tilde{\boldsymbol{\xi}}_{t+1}], \ldots, \mathbb{E}[\tilde{\boldsymbol{\xi}}_{t+H}]$ as our forecast of the future. This is a standard benchmark used in stochastic programming. As above, we implement the time chartering decision made at stage 0 and then roll forward.

### 3.3. Scenario average solution using a multi-scenario stochastic forecast

This approach represents a compromise between relying on the overly simplistic single-scenario deterministic forecast and using the multi-scenario forecast solved as a stochastic program presented above. Given a scenario tree, we obtain optimal time chartering decisions for individual scenarios and combine these decisions into a single time chartering policy by taking a probability-weighted average time chartering solution. We round the average time chartering solution in stage 0, implement this decision, and roll forward.

In practice, business users understand that a mathematical optimization model is an abstraction of reality and therefore make a number of assumptions in order to provide practicable decision support. They also understand that there is uncertainty concerning future economic drivers and parameters. Nevertheless, many business users are more comfortable analyzing a single scenario at a time as opposed to dealing with several scenarios simultaneously, i.e., in a stochastic programming model. In addition, users like the fact that they can compare the optimal solution for each individual scenario with another solution to assess what happens if they were fortunate enough to perfectly predict the future. As a consequence, a typical work process for making time charter decisions is to investigate several single-scenario instances from a set of likely scenarios and then, based on the results, arrive at a decision based on their experience. This approach is clearly ad hoc and is difficult to mimic. Our reason for including the scenario average approach formalized below is to capture a procedure that is similar to what is done today and is computationally reproducible.

Given a scenario tree with $H$ stages and the set of leaf nodes $\mathcal{N}^L$, each path $\mathcal{R}(n)$ for $n \in \mathcal{N}^L$ corresponds to a complete scenario of realizations $(\xi_1, \ldots, \xi_H)$ of the random parameter $\tilde{\boldsymbol{\xi}}$. Let $\mathcal{S}$ denote the set of all scenarios obtained in this way, and $\mathcal{N}^s$ denote the set of nodes of an individual scenario $s$. We solve look-ahead model (9) as a deterministic model for each scenario $s \in \mathcal{S}$, where $\mathcal{N} = \mathcal{N}^s$ and $\pi_n = 1$ for $n \in \mathcal{N}^s$. We denote the time chartering solution obtained as $x^{\text{TC},s}$. We then write $\mathbf{x}^{\text{TC,SA}} = \sum_{s \in \mathcal{S}} \pi_s \mathbf{x}^{\text{TC},s}$, where $\pi_s = \prod_{n \in \mathcal{N}^s} \pi_n$. Since the vector $\mathbf{x}^{\text{TC,SA}}$ may not be integer, we round each component to the nearest integer.

## 4. Instance generation

A "base" instance and a large instance, whose components mimic important elements of a real-world shipping application, were used for our case study. Below we describe their parameters as well as the scenario generation technique we employed in a simulation framework to compare policies.

### 4.1. Base instance characteristics

Fig. 3 shows the components of our base instance, including temporal and topological aspects. There are two loading ports and three discharging ports. For each discharging port, the upper bound on inventory $\overline{S}_{d,t}$, initial inventory $S_{d,0}$, and the steady state demand $\bar{\Delta}_d$ are listed. For this instance only, we assume that all paths are simple roundtrips and therefore the index $p$ may also be interpreted as a loading port-discharging port pair. Associated with each arc is the roundtrip travel time $D_{p,vc,t}$ (in days) between each loading port and discharging port. We assume that this parameter is independent of the vessel class $vc$ and the time period $t$ in which the voyage takes place.

Charter rates are stated in US$/day and reflect rates around the May-August 2013 time frame as provided by Braemar ACM Shipbroking on www.koenig-cie.de/en/content/tanker-charter-rates for the following ships: Suezmax 200 kt, VLCC 250 kt, and VLCC 300 kt.

Table 2 lists the voyage and operating cost $C^{V+O}_{p,vc,t}$ for a vessel of class $vc$ making a roundtrip between a loading and discharging port pair $p$. We assume that this cost is the same in all periods $t \in \mathcal{T}$. Table 3 lists the parameters that are related to each vessel class $vc$: the capacity $Q_{vc}$ (in kt), the minimum time charter cost per day $C^{TC}_{\min}$, the maximum time charter cost per day $C^{TC}_{\max}$, and the number of vessels available $M_{vc,f}$ for each fare class $f$. There are three vessel classes and two fare classes for each vessel class. For this instance, we assume that there are no production limits and no owned vessel fleet.

### 4.2. Large instance characteristics

In addition to the above base instance, we generated a larger instance to further demonstrate the viability and scalability of our approach. Fig. 4 shows the main components of this instance, just as was done above.

There are six loading ports and seventeen discharging ports. To improve readability, a different arc style is used for trips originating from each loading port. Similar to our base instance, we assume that the roundtrip travel time $D_{p,vc,t}$ is independent of the vessel class $vc$ and the time period $t$ in which the voyage takes place. The same three vessel classes described in Table 3 are used in this instance, where the number of vessels available $M_{vc,f}$ for each fare class $f$ is increased to accommodate the demand. Different from our base instance, we introduce production capacities for loading ports. In our computational experiments presented in Section 5.2, the production capacity of LP2 is set to 100,000, LP3 is set to 70,000, and LP4 is set to 80,000 units per period. Consequently, in the computational experiments presented in Section 5.2, discharging ports are not necessarily supplied from the closest loading port. We additionally introduce a fleet of owned vehicles comprised of 30 vessels in vessel class 1, 35 vessels in vessel class 2, and 35 vessels in vessel class 3.

### 4.3. Scenario tree generation

In this section, we discuss the methodology for sampling random parameters and constructing a scenario tree. Following the approach described in Section 4.1 of Bakkehaug et al. (2014), we assume that all random parameters are strongly positively correlated with a so-called *market condition* parameter $m$ and that there is a continuous probability distribution governing $m$. The implication of this "high correlation" assumption is that when the market condition is high (low), demand and chartering costs are high (low). A similar approach was used in Bakkehaug et al. (2014), where a high (low) market condition in period $t$ corresponds to high (low) demand and charter costs in the same period. The ideas described below closely parallel those of Bakkehaug et al. (2014); we present them here for completeness.

Let $t$ be a time period in the future, and let $\mathbb{P}(m_t = m)$ be the probability of market condition having value $m$ in time period $t$, given that we do not know the current market condition. We assume that $\mathbb{P}(m_t = m)$ has a symmetric, bell shaped, truncated probability distribution for $m \in (a, b)$, with mean $\mu$, standard deviation $\sigma$ and lower and upper bounds $a$ and $b$, respectively. Furthermore, we assume that the market condition for the next period follows a truncated normal distribution where $\mu, \sigma, a$ and $b$ are determined by the current market condition. Let $F(m_t)$ be the market condition for period $t+1$ given the current condition $m_t$. Moreover, let $\lambda_\mu = 0.2$ be a multiplier that determines how fast the mean approaches the steady state mean, $\mu$, and $\lambda_\sigma = 0.3$ be a multiplier that determines how fast the standard deviation increases with the distance from steady state mean. Based on the observed market condition $m_t$, we update the mean using

$$\mu = \begin{cases} m_t + \min\{\lambda_\mu(\mu - m_t), \mu - m_t\} & \text{if } m_t < \mu \\ m_t - \min\{\lambda_\mu(m_t - \mu), m_t - \mu\} & \text{if } m_t \geqslant \mu. \end{cases}$$

Further, we write $\sigma = \underline{\sigma} + \lambda_\sigma(m_t - \mu)^2, a = \max\{m_{\min}, m_t - \beta - 1/50\}$ and $b = \min\{m_{\max}, m_t + \beta + 1/50\}$, where $\underline{\sigma}$ is the lowest possible standard deviation for a period, the lowest and the highest market condition are represented by $m_{\min}$

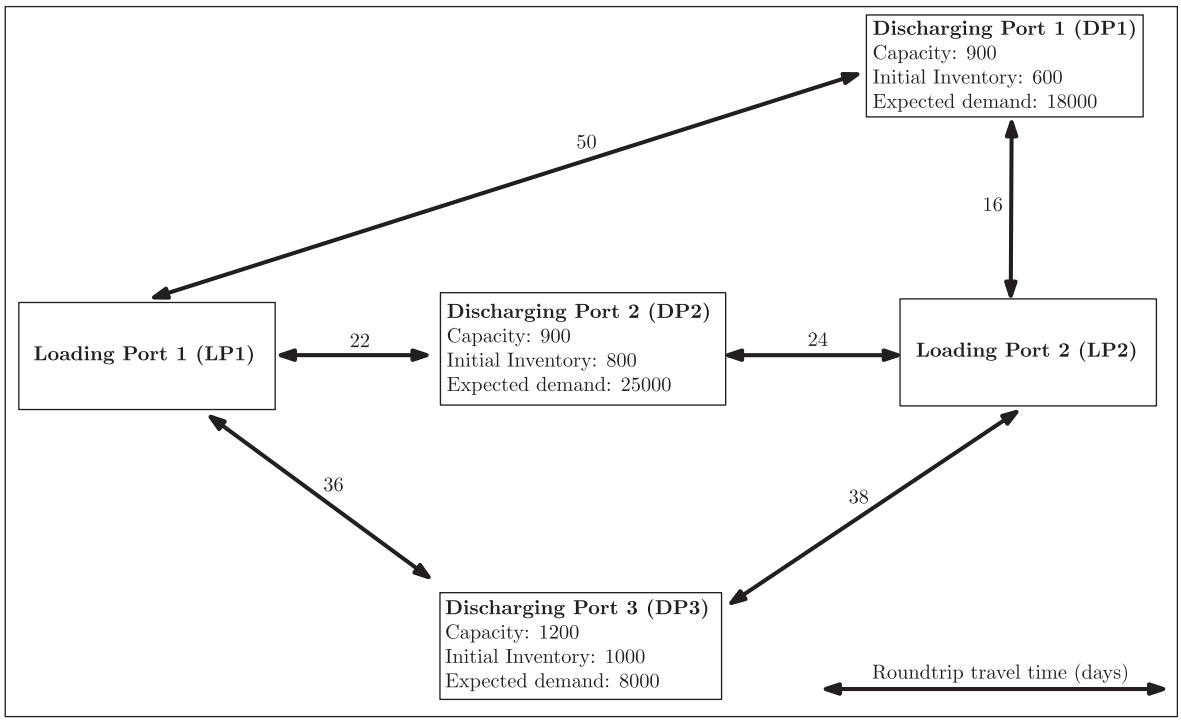


**Fig. 3.** Base instance components.

**Table 2**
Voyage and operating cost parameter $C^{V+O}_{p,vc,t}$ (US$1000/roundtrip) for base instance.

| Vessel Class 1 | | | | Vessel Class 2 | | | | Vessel Class 3 | | | |
|---|---|---|---|---|---|---|---|---|---|---|---|
| | DP1 | DP2 | DP3 | | DP1 | DP2 | DP3 | | DP1 | DP2 | DP3 |
| LP1 | 1225 | 539 | 882 | LP1 | 1400 | 616 | 1008 | LP1 | 1575 | 693 | 1134 |
| LP2 | 392 | 588 | 931 | LP2 | 448 | 672 | 1064 | LP2 | 504 | 756 | 1197 |

**Table 3**
Vessel class related parameters for base instance.

| | $Q_{vc}$ | Vessel Class 1<br>200 | Vessel Class 2<br>250 | Vessel Class 3<br>300 |
|---|---|---|---|---|
| Fare 1 | $C^{TC}_{min}$ | 16,000 | 21,600 | 27,200 |
| | $C^{TC}_{max}$ | 24,000 | 32,400 | 40,800 |
| | $M_{vc,f}$ | 10 | 15 | 15 |
| Fare 2 | $C^{TC}_{min}$ | 24,800 | 38,400 | 45,600 |
| | $C^{TC}_{max}$ | 37,200 | 57,600 | 64,800 |
| | $M_{vc,f}$ | 15 | 25 | 20 |

and $m_{max}$, respectively, and the truncation of the distribution is adjusted by $\beta$. Finally, we have that $F(m_t) \sim N(\mu, \sigma^2)$ and $F(m_t) \in (a, b)$.

To create a scenario tree from this continuous distribution, we employ the discretization technique presented in Bakkehaug et al. (2014). Accordingly, possible market condition values between 0 and 1 are divided into $k$ equally sized subintervals and the midpoint of the interval is taken to represent the market condition $m$ for that node. We let $[k_1, \ldots, k_H]$ denote the number of intervals considered for the market condition in stage $h \in \mathcal{H}$. Recall that stage 0 corresponds to the root node.

The probability of going from a node $n_1$ to a succeeding node $n_2$ is calculated as

$$\mathbb{P}_{n_1,n_2} = \mathbb{P}\left(\underline{i} < F(m_{n_1}) < \bar{i} | a_{n_1} < F(m_{n_1}) < b_{n_1}\right) = \frac{\Phi\left(\frac{\bar{i}-\mu_{n_1}}{\sigma_{n_1}}\right) - \Phi\left(\frac{\underline{i}-\mu_{n_1}}{\sigma_{n_1}}\right)}{\Phi\left(\frac{b_{n_1}-\mu_{n_1}}{\sigma_{n_1}}\right) - \Phi\left(\frac{a_{n_1}-\mu_{n_1}}{\sigma_{n_1}}\right)} \tag{10}$$

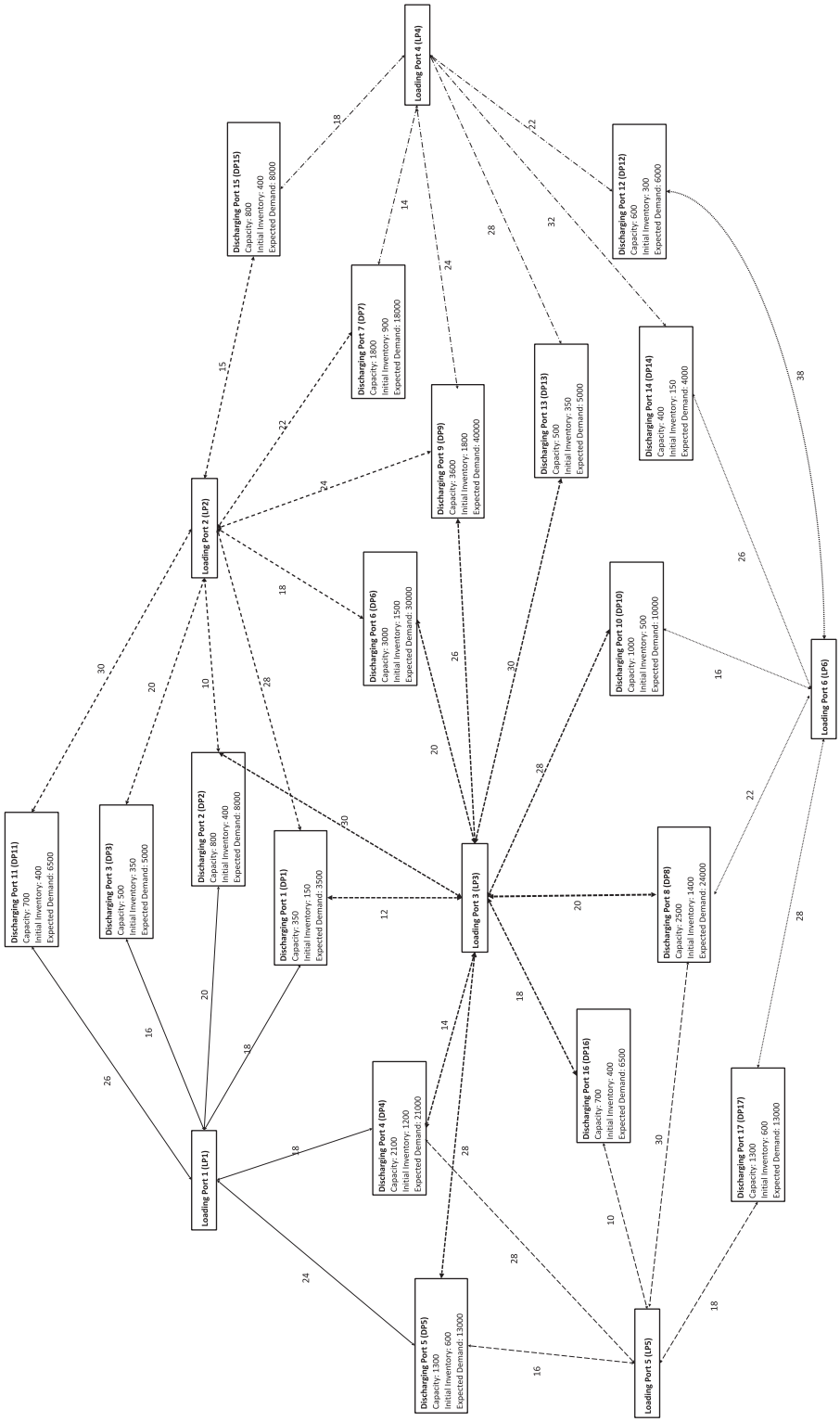


**Fig. 4.** Large instance components.

where $\underline{i}$ and $\bar{i}$ are the lower and upper bounds of the interval represented by node $n_2$, the market condition of node $n_1$ is denoted by $m_{n_1}$, and $\Phi(\cdot)$ is the cumulative standard normal distribution. The probability of node $n \in \mathcal{N}$ is then calculated as $\pi_n = \pi_{a(n)} \mathbb{P}_{a(n),n}$.

We next explain how we generate the random parameters that depend on the market condition. In particular, these parameters are used when making time charter decisions for period $t$, at the end of period $t-1$. Since we assume that time charter decisions are made before the market condition for period $t$ is revealed, see Fig. 1, $m_t$ is not known at this point. In our rolling horizon algorithm, we assume that the time charter cost $C^{\text{TC}}_{l,vc,f,t,t'}$ for each vessel class $vc$ and fare class $f$ is the same for each loading port $l$. We also assume that charter rates exhibit decreasing marginal costs as a function of time to reflect a slight economic incentive for chartering for longer durations. We calculate this parameter using the values $C^{\text{TC}}_{\min}$ and $C^{\text{TC}}_{\max}$ given in Table 3. Accordingly, given two previous market conditions $m_{t-1}$ and $m_{t-2}$, we first forecast a market condition for $t' \geqslant t$. The future market condition is predicted to increase (decrease) if the market condition has increased (decreased) in the past two periods. Mathematically, $m_{t'} = m_{t-1} + 0.01(t'-t+1)$ if $m_{t-1} > m_{t-2}$ and $m_{t'} = m_{t-1} - 0.01(t'-t+1)$, otherwise. With this forecasted market condition, we estimate the single-period time charter cost $C^{\text{TC}}_{vc,f,t',t'+1}$ for vessel class $vc$ and fare $f$ in period $t'$, as $\overline{T}\left(C^{\text{TC}}_{\min} + m_{t'}(C^{\text{TC}}_{\max} - C^{\text{TC}}_{\min})\right)$, where $\overline{T}$ is the duration of a period in days. For $t'' > t'+1$, we assume that a discount is applied according to the formula $\Delta C^{\text{TC}}_{vc,f,t',t'+1} \frac{(t''-t')}{2}$, where $\delta \in (0,1)$ is the discount factor. Therefore, we write $C^{\text{TC}}_{vc,f,t',t''} = C^{\text{TC}}_{vc,f,t',t'+1} - \overline{T}\delta C^{\text{TC}}_{vc,f,t',t'+1} \frac{(t''-t')}{2}$ for $t'' > t'$.

The voyage charter cost $C^{\text{VC}}_{p,vc,t}$ for a voyage between port pair $p$ is assumed to be a function of the single-period time charter cost $C^{\text{TC}}_{vc,1,t',t'+1}$ for vessel class $vc$ in period $t$, the voyage and operating cost $C^{\text{V+O}}_{p,vc,t}$ between port pair $p$ with vessel class $vc$, as well as the market condition $m_t$. We write $C^{\text{VC}}_{p,vc,t} = v\, C^{\text{TC}}_{vc,1,t',t'+1} \frac{D_{p,vc,t}}{\overline{T}}(1+m_t) + C^{\text{V+O}}_{p,vc,t}$, where $v$ is a parameter that describes the relationship between time charter and voyage charter costs.

Finally, to construct the steady state demand forecast $\bar{\Delta}_{d,t}$ for each discharging port $d$ and time period $t$, we assume that it depends on the previous market condition realization. Moreover, we assume that the market condition follows a mean reversion process, i.e., it reverts to the steady state market condition $\mu$ over a set of periods, as follows: $\bar{\Delta}_{d,t} = \bar{\Delta}_d + (\frac{m_{t-1}}{\mu}\Delta_d - \bar{\Delta}_d)\, e^{-\rho t}$, where $\rho$ is a constant parameter that controls how fast the market condition reverts to the steady state $\mu$.

In our computational experiments reported in Section 5, we use $\overline{T} = 90$ (i.e., a time period represents 90 days), $\delta = 0.1, v = 2.5$, and $\rho = 1$. While the company owned fleet is given as input, the initial time charter fleet is not specified; it is chosen by the model.

### 4.4. Illustrative scenario tree example

Fig. 5 illustrates how scenario trees and market condition realizations are generated in a rolling horizon framework. In this example, we present the three-stage subtree (i.e., the first three stages) of a four-period look-ahead scenario tree in each time period $t, \ldots, t+3$. At each stage of the tree, the number of children is equal to 2, with even-numbered children representing a market condition of 0.25, and odd-numbered children representing a market condition of 0.75. We start with an initial observation of the market condition in period $t$, that is $m_t = 0.454$. We update the values $\mu, \sigma, a$ and $b$ as described above. For example, after $m_t = 0.454$ is observed, we obtain $\mu = 0.463$, and $\sigma = 0.13$. The probability of transitioning from each parent node to children nodes is calculated according to Eq. (10). The probability of each node $n$ is then calculated as $\pi_{a(n)}\mathbb{P}_{a(n),n}$, where $\mathbb{P}_{a(n),n}$ is the transition probability from parent node $a(n)$ to $n$. The distribution of $m_{t+1}$ is represented as $N(0.463, 0.13^2)$, where a realization of $m_{t+1} = 0.396$ is observed. Scenario trees for periods $t+1, t+2$ and $t+3$ are obtained similarly. Note that as the sequence of market conditions observed are decreasing, the probability of transitioning from node 0 to node 1, which represents a market condition of 0.25, is increasing.

Fig. 5 also includes an example showing how the time charter costs change after each respective market condition is observed. Here we present the time charter cost projections for a four-period look-ahead algorithm. In each table, we report $C^{\text{TC}}_{l,vc,f,h_1,h_2}$ for vessel class 1 and fare class 1, from the beginning of the time period $t(h_1)+1$ until the end of time period $t(h_2)$, where $h_i$ is a stage and $t(h_i)$ is the time period that corresponds to it. These costs are calculated using the $C^{\text{TC}}_{\min}$ and $C^{\text{TC}}_{\max}$ values for vessel class 1, given in Section 3. The single period time charter cost decreases as a reflection of the decreasing market conditions. Moreover, in each time period, projected time charter costs show a decreasing trend in line with the market development.

After creating a scenario tree, where the market condition $m_n$ and the probability $\pi_n$ of each node $n$ is determined as above, we calculate the demand for each discharging port $d \in \mathcal{D}$ at each node $n$. To this end, we assume that $\bar{\Delta}_{d,t}$ represents the expected demand for discharging port $d$ in period $t$ under the steady state market condition $\mu = 0.5$. Therefore the demand for discharging port $d$ at node $n$ can be calculated as $\frac{m_n}{\mu}\bar{\Delta}_{d,t(n)}$, where $m_n$ is the market condition at node $n$ and $t(n)$ is the time period associated with node $n$.

## 5. Computational experiments and results

In this section, we compare the performance of the three look-ahead policies listed in Table 4, all of which rely on look-ahead model (9). We also compare the policies using different look-ahead horizons and scenario tree configurations. Specifically, we evaluate the policies within a Monte Carlo simulation framework outlined in Algorithm 1. Bakkehaug et al. (2014) completed a thorough evaluation to determine the effect that the scenario tree structure has on policy performance. To distinguish our computational work from theirs, we investigate fewer scenario trees, but instead offer two additional features. First, we evaluate the performance of the scenario average policy (H) and show that it can be quite robust. This is somewhat surprising given that it is producing a suboptimal solution to the actual look-ahead model. Second, we consider a situation in which the forecasted market condition does not follow the same underlying probability distribution as the actual market condition. This is important since, in an actual business environment, one cannot expect to know the underlying probability distribution of many random parameters.

**Algorithm 1.** Rolling Horizon Simulation

1: Initialization: $t = 0$; `simulatedCost = 0`; set actual market condition $m_0$ and initial inventories
2: Solve look-ahead model (9) to determine the initial fleet using forecasted market condition $\hat{m}_0$
3: **for** $t = 1, \ldots, T = 20$ or 40 **do**
4: Update time charter vessel fleet based on acquisitions made in $t - 1$
5: Realize true market condition $m_t$ and stochastic parameters
6: Solve single-period deployment model to satisfy observed demand
7: Create a scenario tree based on a forecasted market condition $\hat{m}_t$
8: Solve look-ahead model (9) using a policy in Table 4. Fix here-and-now time charter decisions $\mathbf{x}_t^{TC}$
9: Add time charter costs and deployment costs to `simulatedCost`
10: **end for**
11: Add to `simulatedCost` the sunset value $R_{T+1}(\mathbf{x}_0^{TC}, \mathbf{x}_1^{TC}, \ldots, \mathbf{x}_T^{TC}, \tilde{\mathbf{C}}_{T+1}^{TC})$ of time chartered vessels remaining in the fleet at the end of the planning horizon.
12: **return** `simulatedCost`

We use the instances described in Sections 4.1 and 4.2. We construct scenario trees using the approach described in Section 4.3 with the steady state market condition $\mu = 0.5$, the minimum standard deviation for a single period $\underline{\sigma} = 0.13$, and the minimum and maximum value of the market condition $a = 0$ and $b = 1$, respectively. We take a period to be 90 days (3 months) and evaluate the performance of each policy over 20 periods (5 years) of simulated market conditions unless otherwise stated. The relative optimality gap is used as our main metric to compare the policies and is calculated by comparing the total simulated cost (i.e., the parameter `simulatedCost` returned in Algorithm 1) of each policy relative to the minimum total simulated cost obtained across all policies. We report our results as an average of 30 replications unless otherwise stated.

We perform all computations using IBM ILOG CPLEX version 12.5 with default parameter settings, on a Windows machine with Windows 7 Professional running a 64-bit x86 processor equipped with 2.83 GHz Intel Core2 Quad Q9500 chips and 4 GB RAM. All implementations were done using the.NET framework with C#. All models are solved either until a 0.1% relative optimality gap is achieved or a time limit of 3600 s is reached.

**Notation and Terminology.** A *scenario tree structure* $[k_1, \ldots, k_H]$ denotes an $H + 1$-stage scenario tree with $k_h$ nodes per parent node in stage $h = 1, \ldots, H$ and whose root node occurs at stage $h = 0$. A decision model or solution approach refers to one of the three items listed in Table 4. A *policy* refers to a solution approach coupled with a specific scenario tree structure. For example, S-7532 is shorthand for a policy based on a five-stage stochastic decision model with a four-period look-ahead horizon having scenario tree structure [7,5,3,2]. A *minimum time charter duration* of $r$ periods (for some fixed positive integer $r$) means that time charter vessels must be chartered for a minimum of $qr$ periods, for any positive integer $q$. For example, a minimum time charter duration of $r = 2$ periods implies that vessels can only be chartered for $2, 4, 6, \ldots$ periods.

### 5.1. Base instance results

#### 5.1.1. Value of scenario based decisions

In our first set of computational experiments, we aim to capture the advantage of using a scenario tree based approach to the fleet sizing and deployment decisions. In this set of experiments, we assume that the distribution given in Section 4.3 represents the true development of market conditions. The maximum time charter duration is 4 periods.

In Fig. 6, we compare four different scenario tree structures with a 4-period look-ahead horizon: $[7, 5, 3, 2]$, $[3, 3, 3, 3]$, $[5, 3, 2, 1]$, and $[1, 1, 1, 1]$. Scenario tree $[1, 1, 1, 1]$ corresponds to a deterministic approach based on the expected value of the market condition and its corresponding policy is D-1111. We solve each scenario tree model, except for $[1, 1, 1, 1]$, using two different approaches. The first is to solve the scenario tree model (9) to exact optimality (S- in Fig. 6),

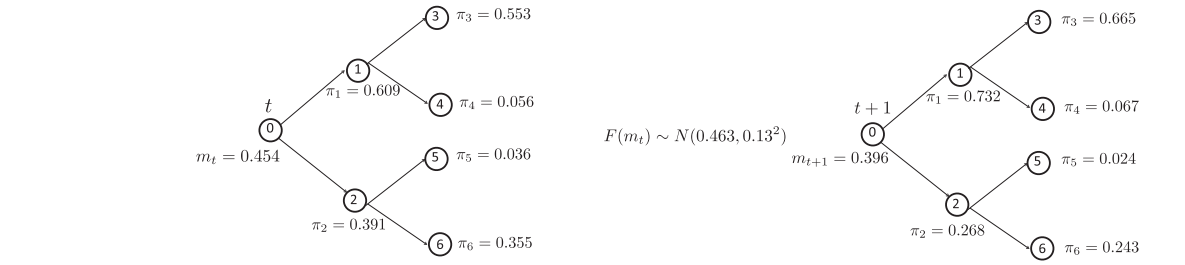


| $h_1 \setminus h_2$ | 1 | 2 | 3 | 4 |
|---|---|---|---|---|
| 0 | 20000 | 38000 | 54000 | 68000 |
| 1 | | 20000 | 38000 | 54000 |
| 2 | | | 20000 | 38000 |
| 3 | | | | 20000 |

| $h_1 \setminus h_2$ | 1 | 2 | 3 | 4 |
|---|---|---|---|---|
| 0 | 19555 | 37222 | 53000 | 66666 |
| 1 | | 19555 | 37111 | 52777 |
| 2 | | | 19444 | 37000 |
| 3 | | | | 19333 |

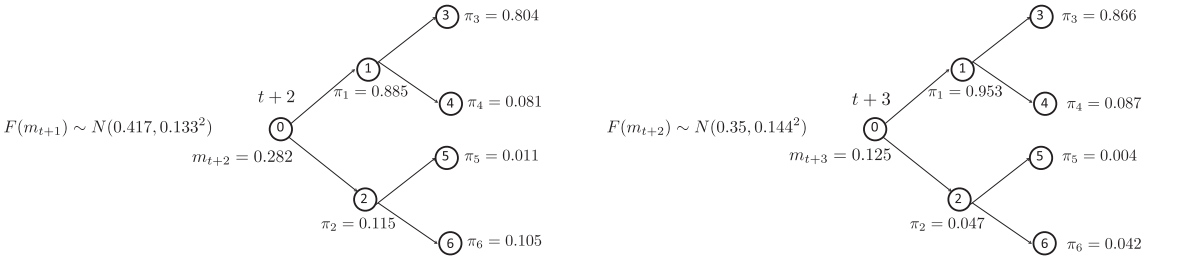


| $h_1 \setminus h_2$ | 1 | 2 | 3 | 4 |
|---|---|---|---|---|
| 0 | 19111 | 36333 | 51666 | 65111 |
| 1 | | 19000 | 36222 | 51555 |
| 2 | | | 19000 | 36111 |
| 3 | | | | 18888 |

| $h_1 \setminus h_2$ | 1 | 2 | 3 | 4 |
|---|---|---|---|---|
| 0 | 18222 | 34666 | 49222 | 62000 |
| 1 | | 18111 | 34444 | 49000 |
| 2 | | | 18000 | 34333 |
| 3 | | | | 18000 |

**Fig. 5.** Example evolution of scenario trees and time charter costs $C^{TC}_{vcf,h_1,h_2}$ for vessel class 1 and fare class 1.

**Table 4**
Solution approaches compared.

| Symbol | Solution approach | Description | Section explained |
|---|---|---|---|
| S | Stochastic | Stochastic programming solution using a multi-scenario stochastic forecast | 3.1 |
| D | Deterministic | Expected value solution using a single-scenario deterministic forecast | 3.2 |
| H | Heuristic | Scenario average solution using a multi-scenario stochastic forecast | 3.3 |

and the second is to solve it heuristically using the averaged scenario solution method (H- in Fig. 6) described in Section 3.3. In Fig. 6, we also explore three different time chartering options in which vessels must be chartered for a minimum number of periods, a requirement that may occur in certain circumstances. The first is the least restrictive and requires a minimum duration of a single period. In this option, vessels can be time chartered for 1, 2, 3, and 4 periods. The second is a minimum duration of two periods, i.e., vessels can be time chartered for 2 or 4 periods. This corresponds to a setting in which a period is three months and time charters are only available in six-month or one-year contracts. Finally, the third option is a minimum duration of four periods, i.e., vessels can only be time chartered for 4 periods or in one-year contracts.

For each chartering option and policy, Fig. 6 summarizes the optimality gap obtained across 30 replications. Here the optimality gap is calculated by comparing the total cost of each policy to the minimum total cost obtained across all seven approaches. On each box of the box-and-whiskers plot in Fig. 6, the central mark is the median, the edges of the box are the 25th and 75th percentiles, the whiskers extend to the most extreme data points not considered outliers, and outliers are plotted individually. As can be clearly seen in each plot, the scenario tree model with $[7, 5, 3, 2]$ tree structure has the smallest median optimality gap among all policies for each minimum time chartering option. Moreover, for each scenario tree and minimum time charter duration, the exact solution method (S- in Fig. 6) outperforms the heuristic solution method (H- in Fig. 6). Our results also show the advantage of scenario based policies over deterministic ones. In particular, when the minimum time charter duration is a single period, the average optimality gap for the stochastic look-ahead S-7532 is 2.41%,

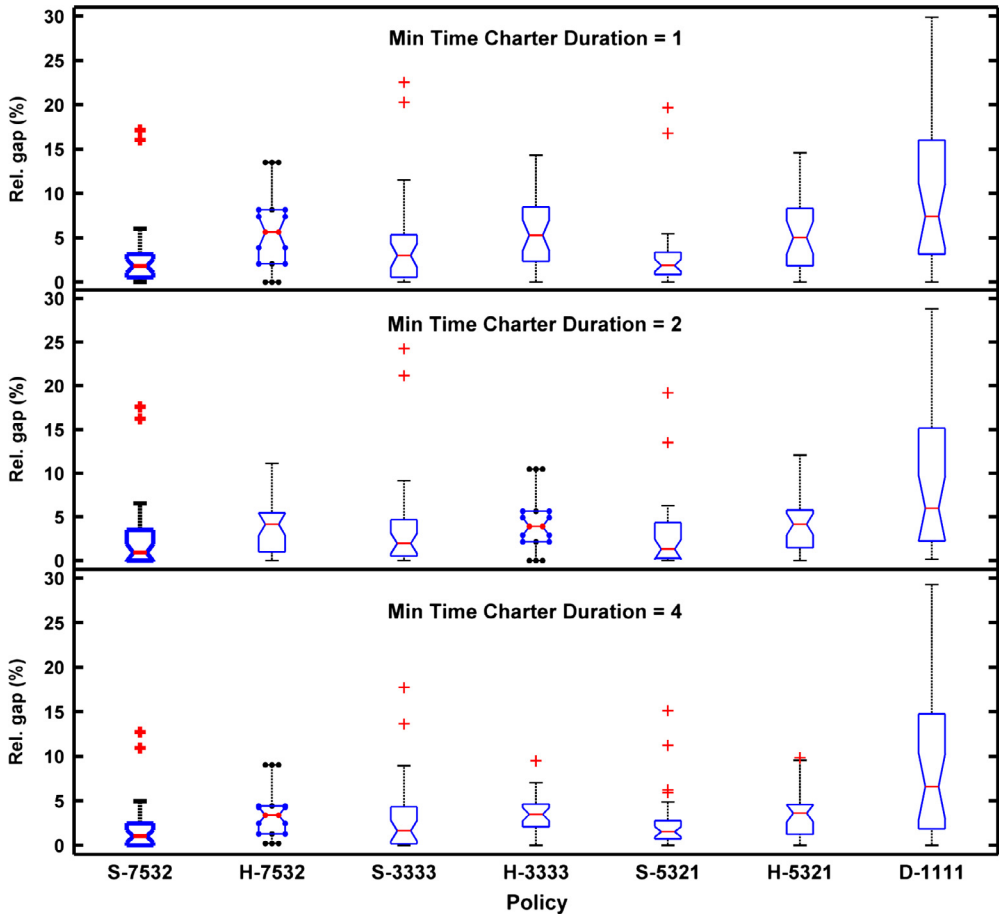


**Fig. 6.** Relative optimality gap comparison of different policies with the same time charter duration.

whereas the average optimality gap for the deterministic policy D-1111 is 10.24%. Similar results are observed for each minimum time charter duration.

It should be noted that the two worst cases (outliers) for the scenario tree policies correspond to simulation runs in which the actual market condition stayed very low, never reaching the expected long-term/steady-state market condition of 0.5. Consequently, the stochastic look-ahead continually chartered more vessels compared to the scenario average solution to hedge against a possible rise in the market condition, a scenario which never manifested itself. These two simulation trials indicate that the current stochastic look-ahead may not be beneficial in economic environments with a perpetually low market condition since there is no recourse action when the acquired vessel fleet capacity exceeds the capacity needed to satisfy demand. If these two simulation trials are excluded, the stochastic look-ahead results in superior cost savings and is clearly the best policy.

It is instructive to understand the difference in the time charter decisions generated by the various policies. Fig. 7 compares the fleet evolution in terms of capacity (Mt) for each vessel class (i.e., fare classes are aggregated for each vessel class) in each time period for the stochastic policy S-7532 and the deterministic policy D-1111 when there is a 4-period minimum time charter requirement. The stochastic policy results in significantly (1.5 times, on average) more time charter capacity than its deterministic counterpart. This trend appears consistently across all experiments as the stochastic policy is able to "see" potentially challenging scenarios and pays the upfront cost of time chartering additional vessels in order to save future voyage charter costs when they are unfavorable. This result is also consistent with the one found in Fig. 9 of Bakkehaug et al. (2014) where the best stochastic scenario tree structure resulted in 50% more capacity than the best deterministic tree structure.

### *5.1.2. Impact of different minimum time charter durations*

The results presented in Fig. 6 assume that the minimum time charter duration is given for each policy and compares only the decisions obtained for the same minimum time charter duration with each other when calculating the average optimality gap. However, if the decision maker is able to control the minimum time charter duration, then a natural question is

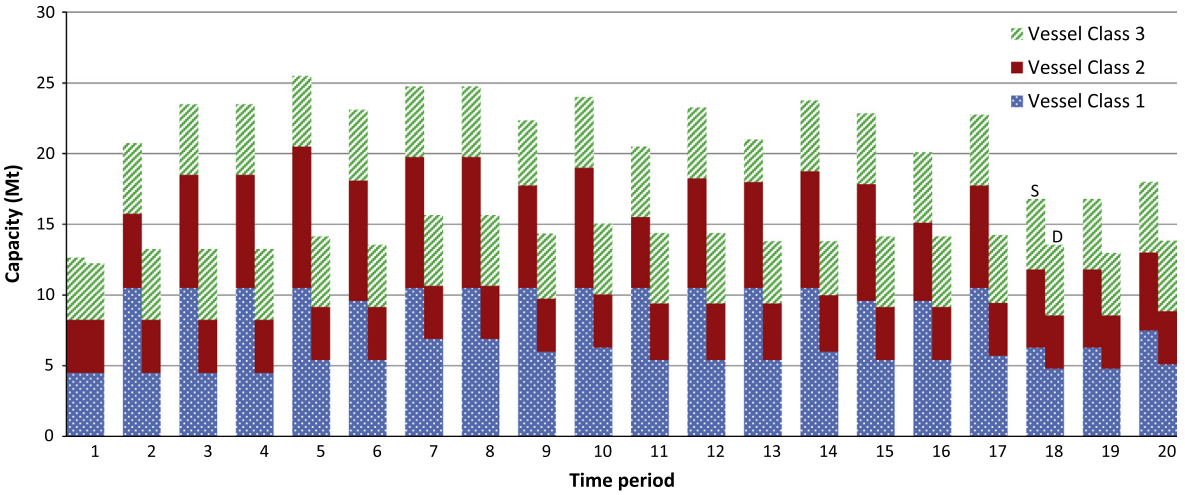


**Fig. 7.** Fleet evolution comparison of S-7532 (left bar) and D-1111 (right bar) with a 4-period minimum time charter requirement.

whether short-term or long-term contracts are more beneficial. Table 5 compares the performance of each policy with respect to different minimum time charter durations, where the average optimality gap of each policy is given under the header "Avg" and the standard deviation is given under the header "StD". The optimality gap in this case is calculated by comparing the total cost of each policy with different time charter durations to the minimum total cost obtained across all policies and minimum time charter durations.

As can be seen in Table 5, the stochastic look-ahead S-7532 with single period minimum time charter duration performs superior to all other policies. It is however not clear from these results that the flexibility of shorter duration time charters will always lead to cost savings. In particular, for the scenario average policy (H), the average optimality gap increases as the minimum time charter duration decreases. One thing to keep in mind when interpreting these results is that our time charter cost construction encourages longer time charter durations. Moreover, when the minimum time charter duration is a single period or two periods, it is still possible to charter vessels for four periods. Therefore, it is not always clear that the single period time charter option will be utilized and be beneficial.

*5.1.3. Impact of different look-ahead horizons*

Results reported in Sections 5.1.1 and 5.1.2 consider a 4-period look-ahead model. In this section, we investigate the effect of the length of the look-ahead horizon on the fleet sizing and deployment decisions since one would expect longer look-aheads to result in better decisions. In particular, we compare the total cost of 3-, 4-, 5-, and 6-period look-ahead horizons, with one-, two-, and four-period minimum time charter durations. We use the scenario tree structures [3,3,3], [3,3,3,3], [3,3,3,3,3], and [3,3,3,3,3,3] for the stochastic policies (S and H), whereas [1,1,1], [1,1,1,1], [1,1,1,1,1], and [1,1,1,1,1,1] tree structures are used for the deterministic policy (D). In order to make a fair comparison, we use the same set of simulated market conditions over 20 periods for all policies. We report our results as an average of 30 replications in Fig. 8.

As expected, longer look-ahead horizons lead to smaller optimality gaps, on average, for all policies. In general, a stochastic look-ahead policy (S) with a 6-period look-ahead does best, i.e., it has the smallest mean optimality gap. For a minimum time charter duration of 4 periods, the mean optimality gap for S-33333 and S-333333 are 1.78 and 1.79, respectively. Interestingly, the average scenario heuristic with the longest look-ahead (H-333333) is the policy with the smallest maximum optimality gap, meaning that over all 30 replications, it had the best worst-case performance. This is evident in Fig. 8 as there are no large outliers (marked with +) for H-333333. One possible explanation for this is that the heuristic method (H) is more cautious compared to the scenario tree model while still considering the uncertainty in the future. The scenario tree model (S) performs worst if the market condition remains very low for a number of periods (especially after a high market condition is observed) because it sees the high market condition as a sign that the demand is going to rise and, as a consequence, time charters a large number of vessels to avoid paying the high price of voyage charters (a scenario that never manifests itself and leads to a waste of capital). On the other hand, the scenario average model (H) averages decisions under high market conditions with those under low market conditions and time charters fewer vessels compared to the scenario tree model. Of course, one could make the scenario tree model (S) more conservative by introducing a risk-aversion component, e.g., conditional value-at-risk, into the objective function.

*5.1.4. Policy comparison with inaccurate forecasts*

Just as it is common and proper when doing statistical fitting to perform cross validation, i.e., retaining a subset of the data used to fit the model to test the performance of the fit, we apply our computational experiments in situations where the true market condition (as determined by the "simulator") does not necessarily agree with the forecasted market

**Table 5**
Average optimality gap (%) comparison of policies with different minimum time charter durations.

| | Minimum time charter duration | | | | | |
|---|---|---|---|---|---|---|
| | 1-period | | 2-period | | 4-period | |
| Policy | Avg | StD | Avg | StD | Avg | StD |
| S-7532 | **2.79** | 4.08 | **3.29** | 4.30 | **3.44** | 4.39 |
| H-7532 | 5.52 | 3.79 | 4.76 | 3.07 | 4.63 | 2.37 |
| S-3333 | 4.49 | 5.55 | 4.56 | 5.61 | 4.45 | 5.21 |
| H-3333 | 5.64 | 3.96 | 4.81 | 2.70 | 4.88 | 2.52 |
| S-5321 | 3.11 | 4.41 | 3.51 | 4.11 | 3.98 | 4.64 |
| H-5321 | 5.27 | 4.05 | 4.76 | 3.24 | 4.70 | 2.55 |
| D-1111 | 10.65 | 8.78 | 10.42 | 8.66 | 10.77 | 8.79 |

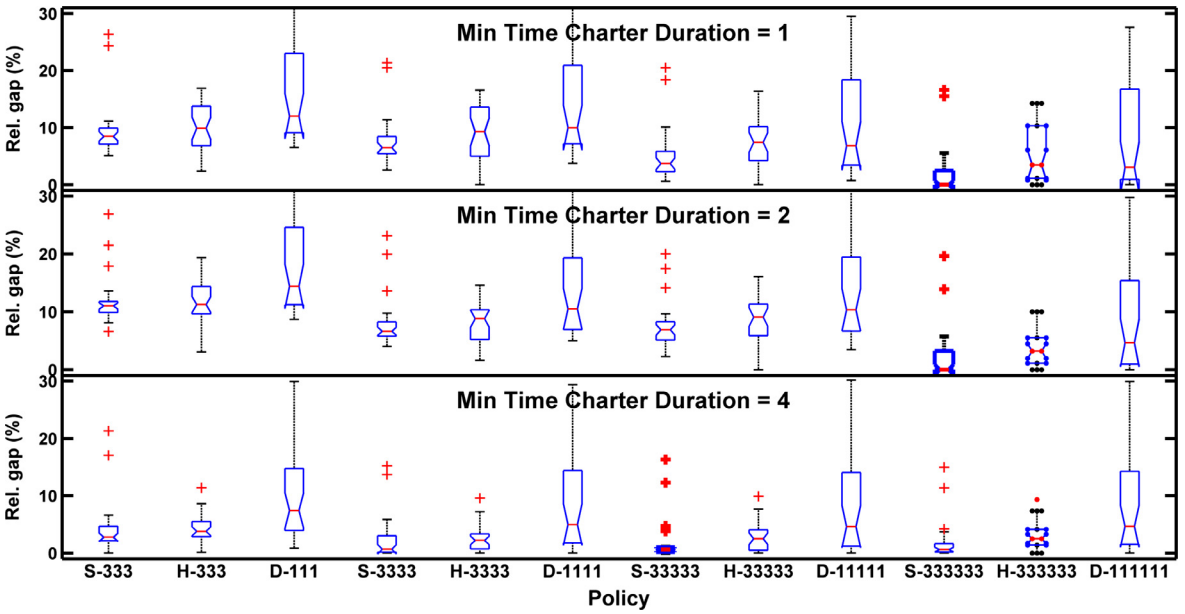


**Fig. 8.** Relative optimality gap comparison of policies using different look-ahead horizons.

condition used to construct the scenario tree. Pantuso et al. (2016) also included such experiments. To this end, we consider two cases. In the first, we assume that the realized market condition is always above the forecasted market condition (header "High" in Table 6). In the second, we assume that the realized market condition is always below the forecasted market condition (header "Low" in Table 6). We let $m_t = \hat{m}_t + U(0, 0.1)$ for the first case and $m_t = \hat{m}_t - U(0, 0.1)$ for the second, where $m_t$ is the realized market condition, $\hat{m}_t$ is the forecasted market condition, and $U(0, 0.1)$ is the standard uniform distribution with lower bound 0 and upper bound 0.1. For this set of experiments, we consider only a minimum time charter duration of four periods. We present our results in Table 6, where the average and the standard deviation of the optimality gap is reported under headers "Avg" and "StD", respectively. Our results show that, when the market condition is higher than expected, the stochastic look-ahead model S-7532 is superior to all other policies. On the other hand, when the market condition is lower than expected, the scenario average policy H-7532 performs best. In this case, it is also true that, in general, scenario average solutions perform better compared to their scenario tree solution counterparts. The reason is that the scenario average policy tends to charter less capacity, which in this case pays off, since the market condition usually remains very low. On the other hand, the scenario tree solutions always hedge against the possibility of the market condition going up. In this case, since there is no recourse for underutilized capacity, the scenario tree solutions incur a higher cost.

*5.1.5. Timing comparison*

In this section, we compare the computation time required to solve each decision model with different scenario trees and different look-ahead horizons for our base instance. In particular, we compare the computation time of 3-, 4-, 5-, and 6-period look-ahead horizons, with one-, two-, and four-period minimum time charter durations. We use the scenario tree structures [3,3,3], [3,3,3,3], [3,3,3,3,3], and [3,3,3,3,3,3] for the stochastic policies (S and H), whereas [1,1,1], [1,1,1,1],

**Table 6**
Optimality gap (%) comparison when the actual market condition is higher ("High") or lower ("Low") than the forecasted market condition.

| | Actual market condition | | | |
|---|---|---|---|---|
| | High | | Low | |
| Policy | Avg | StD | Avg | StD |
| S-7532 | **0.76** | 1.04 | 4.62 | 3.28 |
| H-7532 | 6.02 | 2.55 | **1.76** | 2.12 |
| S-3333 | 2.42 | 2.59 | 5.07 | 4.91 |
| H-3333 | 9.70 | 2.98 | 1.78 | 1.78 |
| S-5321 | 1.30 | 1.42 | 5.04 | 4.03 |
| H-5321 | 6.31 | 2.88 | 1.82 | 2.28 |
| D-1111 | 17.31 | 9.98 | 6.56 | 6.76 |

[1,1,1,1,1], and [1,1,1,1,1,1] tree structures are used for the deterministic policy (D). We report our results, as an average of the results obtained with different minimum time charter durations, in Fig. 9.

As can be seen in Fig. 9, the stochastic decision model (S) requires the most amount of time, whereas the deterministic model (D) requires the least. On average, solving the scenario tree model (9) exactly (S) requires 10 times more computation time than solving it heuristically (H). This is expected since the scenario tree model considers all future realizations of the market condition simultaneously, whereas the heuristic model considers each scenario individually.

Another observation evident from the results of Fig. 9 is that as the look-ahead horizon increases, the solution time required for the stochastic (S) and heuristic (H) models increases significantly, whereas the solution time for the deterministic model (D) does not significantly change. In general, for decision model (S) the solution time increases exponentially in the number of periods of the look-ahead horizon. On the other hand, the scenario average model (H) shows slight exponential growth in the number of periods of the look-ahead horizon. We expect that the solution time required for both models would increase drastically in the number of periods of the look-ahead horizon if the deployment decision variables are required to be integer, or the detailed routing decisions are considered.

Next, Table 7 compares the average solution time of each decision model with a 4-period look-ahead horizon and different scenario trees. We only report our results for the stochastic solution methods (S and H), since the deterministic method is not affected by the scenario tree structure. We use the scenario tree structures [3,3,3,3], [5,3,2,1], and [7,5,3,2].

Table 7 suggests that the solution time is linear in the number of scenario tree nodes for both decision models. For example, the number of nodes in scenario tree structures [5,3,2,1], [3,3,3,3], and [7,5,3,2] is 80, 120, and 357, respectively, and the solution time for scenario tree structure [5,3,2,1] is roughly 2/3 times that of [3,3,3,3] and 1/3 times that of [7,5,3,2].

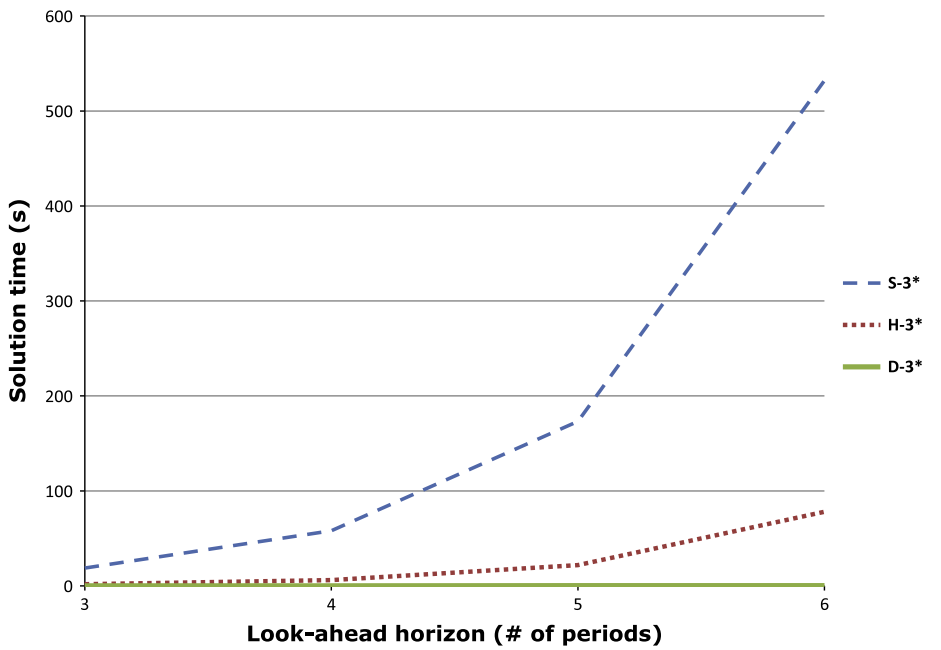


**Fig. 9.** Comparison of average time to solve each decision model as a function of the look-ahead horizon.

**Table 7**
Comparison of average computation time (s) for different scenario tree structures with a 4-period look-ahead.

| Policy | Scenario tree structure | | |
|---|---|---|---|
| | [3,3,3,3] | [5,3,2,1] | [7,5,3,2] |
| S | 57.67 | 38.40 | 172.21 |
| H | 5.16 | 1.97 | 14.70 |

The computational experiments reported here only consider a network involving two loading ports and three discharging ports as shown in Fig. 3. Increasing the number of ports will certainly increase the computation time. However, we expect that the impact would not be as significant as considering detailed routing of vessels.

### 5.2. Large instance results

#### 5.2.1. Value of scenario based decisions

In this section, we repeat our computational experiment from Section 5.1.1 with our large instance to demonstrate the validity of our main conclusions as the problem size grows. In general, we find that the stochastic policies have the potential to offer an uplift of greater than 10%, on average, relative to deterministic policies, and greater than 20% in some extreme cases.

Fig. 10 compares three different minimum time chartering options and four different scenario tree structures with a 4-period look-ahead horizon: $[7,5,3,2]$, $[3,3,3,3]$, $[5,3,2,1]$, and $[1,1,1,1]$. Scenario tree $[1,1,1,1]$ corresponds to a deterministic approach based on the expected value of the market condition and its corresponding policy is D-1111. We solve each scenario tree model, except for $[1,1,1,1]$, using two different approaches. The first is to solve the scenario tree model (9) to exact optimality (S- in Fig. 10), and the second is to solve it heuristically using the averaged scenario solution method (H- in Fig. 10) described in Section 3.3. We report our results for 30 replications as is done in Section 5.1.1.

Fig. 10 reveals that scenario based methods outperform the deterministic approach across all different minimum time charter durations, both on average and in terms of the distribution of the optimality gap. Indeed, for a minimum time charter duration of 1 or 2 periods, we see an uplift of 11–12% from using stochastic policy S-7532 over a deterministic one. Meanwhile, policy S-5321 performs best when the minimum time charter duration is 4 periods. It is also worth noting that the deterministic method has close to 20% optimality gap in some of the replications. Additionally, the average optimality gap for the deterministic approach D-1111 is higher than the worst case of scenario method S-7532.

#### 5.2.2. Longer look-ahead horizons

Our results in Section 5.2.1 showcase the applicability of our approach to realistically-sized instances with a 4-period look-ahead horizon. It is also worth exploring the limits of our approach as the look-ahead horizon increases leading to a

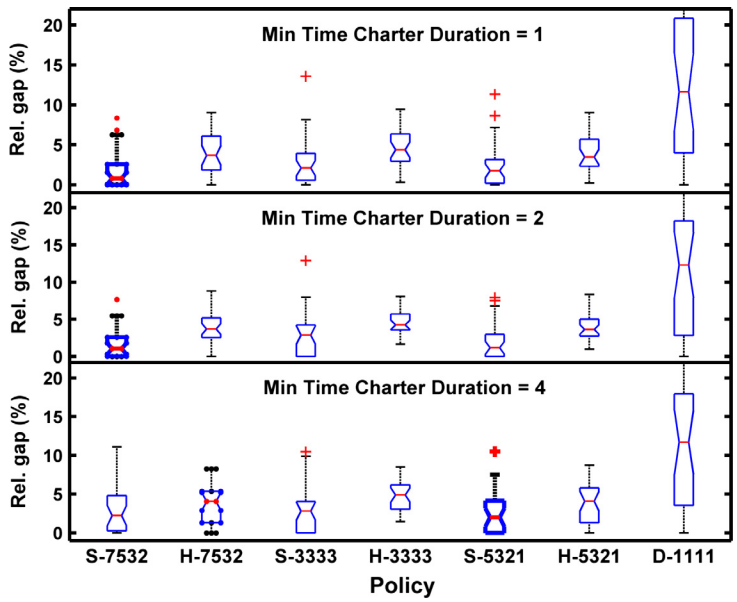


**Fig. 10.** Relative optimality gap comparison of different policies with a 4-period look-ahead and different minimum time charter durations.

**Table 8**
Comparison of average computation time (s) for a single solve for different scenario tree structures and look-ahead horizons.

| Tree structure | # Nodes | # Scenarios | Tree time | S-time | H-time | Speedup |
|---|---|---|---|---|---|---|
| [3, 3, 3, 3, 3, 3] | 1092 | 729 | 0.87 | 291.64 | 119.81 | 2.43 |
| [3, 3, 3, 3, 3, 3, 3] | 3279 | 2187 | 2.39 | 5737.89 | 565.45 | 10.15 |
| [3, 3, 3, 3, 2, 2, 1, 1] | 1254 | 324 | 1.01 | 666.77 | 86.05 | 7.75 |
| [3, 3, 3, 3, 2, 2, 2, 2] | 2550 | 1296 | 17.36 | 6115.86 | 520.43 | 11.75 |
| [5, 3, 2, 2, 1, 1, 1, 1] | 350 | 60 | 0.30 | 30.65 | 12.32 | 2.49 |
| [5, 3, 2, 2, 2, 2, 2, 2] | 1910 | 960 | 1.53 | 2805.96 | 392.26 | 7.15 |
| [7, 5, 3, 2, 1, 1, 1, 1] | 1197 | 210 | 11.28 | 497.20 | 60.31 | 8.24 |
| [7, 5, 3, 2, 2, 1, 1, 1] | 1617 | 420 | 1.44 | 1873.73 | 209.21 | 8.96 |

larger scenario tree size. To this end, we first explore the effects of increasing the look-ahead horizon and the tree size on the solution time of scenario based models. We summarize our results in Table 8 where we present the scenario tree structure used (under the heading "Tree structure"), number of nodes ("# Nodes"), number of scenarios ("# Scenarios"), computational time for building the scenario tree ("Tree Time"), solution time for the scenario tree model ("S-Time"), solution time for the scenario average model ("H-Time"), and the speedup ("Speedup") from using the scenario average model over the scenario tree model computed as S-Time/H-Time. The time reported here is for a single iteration of Algorithm 1. As can be seen from this table, for an 8-period look-ahead solving the scenario tree model can be quite challenging for some scenario tree structures. In fact, for the $[3, 3, 3, 3, 2, 2, 2, 2]$ tree it took more than an hour and a half to build the mathematical model and solve it. It should also be noted that for some scenario trees (e.g., $[3, 3, 3, 3, 3, 3, 3, 3]$) default CPLEX memory limitations were not sufficient to store the branch-and-bound tree and the solution process was aborted. It is clear from this analysis that if the scenario tree model is to be used with longer look-ahead horizons then building the scenario tree should be done more strategically. This analysis also showcases the advantage of the scenario average approach over the scenario tree approach and underscores the importance of developing heuristics that provide good solutions. The scenario average method allows us to analyze many scenarios without having to deal with memory limitations.

Fig. 11 compares four different scenario tree structures with an 8-period look-ahead horizon: $[7, 5, 2, 2, 1, 1, 1, 1]$, $[3, 3, 3, 3, 3, 1, 1, 1, 1]$, $[5, 3, 2, 2, 1, 1, 1, 1]$, and $[1, 1, 1, 1, 1, 1, 1, 1]$. Results are presented for both the scenario tree approach (S-) and the scenario average approach (H-) for each of the scenario trees except for $[1, 1, 1, 1, 1, 1, 1, 1]$. The minimum time charter duration is two periods meaning that vessels can be chartered for 2, 4, 6, or 8 periods. We evaluate the performance of each approach over 40 periods of simulated market conditions and report the results of 10 replications. Similar to our previous results, here again scenario based decision methods perform significantly better than the deterministic approach. However, in contrast to our previous results, increasing the size of the scenario tree does not improve the performance of the scenario tree approach. This is especially evident when comparing policies S-75221111 and H-75221111 where the scenario average approach performs better than the scenario tree approach. It should be noted that with a solution time limit of one hour some iterations of the scenario tree model were not solved to provable optimality possibly leading to the implementation of suboptimal policies. In contrast, the policies obtained from the scenario average model lead to overall better performance.

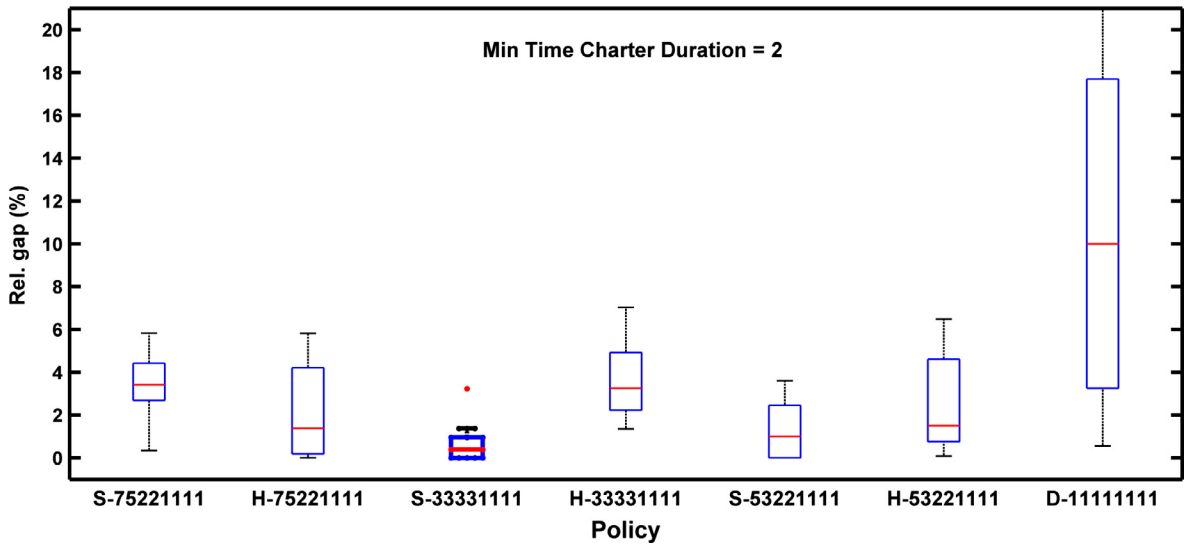


**Fig. 11.** Relative optimality gap comparison of different policies with an 8-period look-ahead.

Finally, we perform a computational experiment with a 12-period look-ahead horizon using the scenario tree structure $[3, 3, 3, 3, 2, 2, 2, 2, 1, 1, 1, 1]$ with a minimum time charter duration of 4 periods. We compare the performance of the scenario average approach to that of the deterministic approach over 40 periods of simulated market conditions and 10 replications. Overall, the scenario average approach had an average optimality gap of 4.27% and a standard deviation of 6.21% whereas the deterministic approach had an average optimality gap of 13.21% and a standard deviation of 12.26%. This experiment shows that the scenario average approach can be used for much longer look-ahead horizons and clearly outperforms the deterministic approach. The scenario average approach can be used with larger scenario trees as well. Here, we choose to use a smaller tree for the sake of computational time as we perform 40 iterations of Algorithm 1 for each replication. In fact, it took an entire week to complete 10 replications for this experiment. However, in a practical business application, the decision maker will likely only perform an iteration of Algorithm 1 every few months and therefore can probably tolerate longer solution times especially those associated with a larger scenario tree.

#### 5.2.3. Discussion

In light of our results in Section 5.2.2, it is natural to ask: How would one handle (i.e., model or solve) a situation in which a high temporal resolution is desired and time charter durations of multiple years are possible? For instance, consider an application in which one would like to model quarterly decisions for five years. Without any alterations, this would require a 20-period look-ahead in our current framework, and, would most likely be very difficult to solve using our stochastic policy. There are at least two logical and practical options to regain computational tractability: reduce the temporal resolution or reduce the distributional resolution. We discuss both options below.

From a modeling perspective, one could use the framework of our existing model, but approximate future decisions with a more coarse-grained resolution by having future time periods represent longer durations of time. For example, using an 8-period lookahead, one could use our framework to allow for time charter durations up to five years as follows. One could represent the first year with four periods so that the first four time periods correspond to quarterly decisions (i.e., decisions made every three months) and the last four periods correspond to annual decisions (i.e., time period $t = 5$ represents a decision for year 2, $t = 6$ a decision for year 3, $t = 7$ a decision for year 4, and $t = 8$ a decision for year 5. Quarterly data for the last four years would need to be aggregated so that the parameters given to our model would represent the correct duration (e.g., annual demand as opposed to quarterly demand). Clearly, this approach sacrifices temporal resolution in hopes that an optimization solver will produce meaningful results.

From an algorithmic perspective, one could use a sampling-based approach or a scenario clustering approach so that the same temporal resolution is maintained, but with less distributional resolution of future uncertainty. Sample average approximation (SAA) is a popular approach that would keep the spirit of our approach (Kleywegt et al., 2002). While it does not provide deterministic optimality guarantees, it does allow one to compute statistical guarantees. Suppose there were $3^{20}$ scenarios in the aforementioned example. SAA would take a subset of these scenarios, say, 1000 so that the scenario policy could be solved to provable optimality in a reasonable amount of time. One could then replicate this experiment multiple times by sampling another 1000 scenarios and re-solving. One uses the results from these multiple replications to choose a decision to implement for the here-and-now decision.

Both approaches have their own merits. However, theoretical results already exist to indicate that sampling methods are likely inadequate to solve multi-stage stochastic programs with many stages. Indeed, Shapiro and Nemirovski (2005) concluded that the number of samples required to approximate multi-stage stochastic programs to reasonable accuracy grows exponentially with the number of stages. As a partial remedy, we showed that the scenario average heuristic is useful and practical in this situation, allowing a decision maker to evaluate many scenarios without the formidable time investment and memory issues.

## 6. Conclusions and future research opportunities

We introduce a fleet sizing problem in industrial bulk shipping and provide the first multi-stage stochastic programming look-ahead model for it, which can be used for tactical planning or for planning at the interface of the strategic and tactical level. In so doing, we demonstrate the potential benefits of explicitly incorporating parameter uncertainty into a decision support framework with the maritime sector. Indeed, a stochastic look-ahead approach always outperforms a deterministic look-ahead when the same look-ahead horizon is considered.

It is instructive to describe our empirical conclusions in comparison with those of Bakkehaug et al. (2014). Although their problem has a longer planning horizon (15 years with annual decisions vs. 5 years with quarterly decisions) and pertains to liner shipping, the reliance on solving a multi-stage stochastic program using different scenario trees is similar. One would expect there to be many commonalities in the empirical findings. For the most part, our conclusions agree. We both find that stochastic look-ahead policies provide savings. They report a 4% decrease in total costs from using their best stochastic look-ahead over the simplest deterministic policy (D-1 using our notation). We found that this reduction could be as large as 12%, on average, in our problem setting. This could be due to the fact that their problem allowed for out-chartering, an additional recourse option in low market conditions not considered in our setting. Our results also agree with their conclusion that "it is more important to model the uncertainty of the near future with more details than it is for the later stages" (Bakkehaug et al., 2014, p. 73). Perhaps the most notable difference is that we observed what one would expect: The longer the look-ahead

horizon, the better the performance, i.e., the lower the average total simulated cost. This holds for any policy, regardless of the scenario tree structure. On the contrary, they found that a longer look-ahead was not always met with lower costs (e.g. see scenario tree 15 vs. 18 in Table 4 of Bakkehaug et al., 2014).

There are several fruitful directions that we encourage the research community to pursue:

- While we have focused exclusively on tactical in-chartering decisions for fleet renewal because of its importance to our particular setting, it might be interesting to include these decisions within a larger strategic problem in which vessels are also purchased and decommissioned.
- In this work, we only considered uncertain demand. It would be interesting to investigate the effects of uncertain supply and other parameters. Uncertain supply was not a significant issue in this application, but it could be in other settings.
- From a computational perspective, an open question is: What is the impact of including detailed routing decisions on chartering decisions? Inclusion of such detail will almost certainly require decomposition schemes and, therefore, even more effort to implement in practice. Of course, this question falls under a much larger umbrella in the engineering community related to multi-scale modeling where one has to forgo certain details within a mathematical model in order for it to be computationally tractable.
- From a methodological perspective, an open question is: At what point does the scenario tree become intractable for commercial solvers to solve the stochastic program in extensive form? Our solution methods rely on commercial mixed-integer programming solvers. It would be interesting to explore specialized algorithms for solving multi-stage stochastic integer programs. For example, a progressive hedging scheme coupled with tabu search was proposed as a general purpose solver for such problems in Løkketangen and Woodruff (1996).

## Acknowledgments

We thank Giovanni Pantuso for his thorough reading of an early manuscript and his incisive comments that improved the contributions of this paper. We also wish to thank three anonymous referees for their helpful feedback, which strengthened the quality of this paper.

## References

Alvarez, J.F., Tsilingiris, P., Engebrethsen, E.S., Kakalis, N.M.P., 2011. Robust fleet sizing and deployment for industrial and independent bulk ocean shipping companies. INFOR 49 (2), 93–107.
Bakkehaug, R., Eidem, E.S., Fagerholt, K., Hvattum, L.M., 2014. A stochastic programming formulation for strategic fleet renewal in shipping. Transport. Res. Part E: Logist. Transport. Rev. 72, 60–76.
Ben-Tal, A., El Ghaoui, L., Nemirovski, A., 2009. Robust Optimization. Princeton University Press.
Bojović, N., Milenkovic, M., 2008. The best rail fleet mix problem. Oper. Res. 8 (1), 77–87.
Branch, A.E., 2007. Elements of Shipping. Routledge.
Cheon, M.-S., Furman, K.C., Shaffer, T.D., 2012. A modeling framework for railcar fleet sizing in the chemical industry. Indust. Eng. Chem. Res. 51 (29), 9825–9834.
Christiansen, M., Fagerholt, K., Nygreen, B., Ronen, D., 2007. Maritime Transportation. In: Barnhart, C., Laporte, G. (Eds.), Transportation, Handbooks in Operations Research and Management Science, vol. 14. Elsevier, pp. 189–284.
Christiansen, M., Fagerholt, K., Nygreen, B., Ronen, D., 2013. Ship routing and scheduling in the new millennium. Eur. J. Oper. Res. 228 (3), 467–483.
Fagerholt, K., Christiansen, M., Hvattum, L.M., Johnsen, T.A., Vab, T.J., 2010. A decision support methodology for strategic planning in maritime transportation. Omega 38 (6), 465–474.
Fagerholt, K., Rygh, B., 2002. Design of a sea-borne system for fresh water transport – a simulation analysis. Belgian J. Oper. Res. Stat. Comput. Sci. 40, 137–146.
García, C.E., Prett, D.M., Morari, M., 1989. Model predictive control: theory and practice – a survey. Automatica 25 (3), 335–348.
Georghiou, A., Wiesemann, W., Kuhn, D., 2011. The decision rule approach to optimisation under uncertainty: methodology and applications in operations management. Math. Program. 1, 1–40.
Halvorsen-Weare, E.E., Fagerholt, K., 2011. Robust supply vessel planning. In: Pahl, J., Reiners, T., Voß, S. (Eds.), Network Optimization, Lecture Notes in Computer Science, vol. 6701. Springer, Berlin Heidelberg, pp. 559–573.
Halvorsen-Weare, E.E., Fagerholt, K., Nonås, L.M., Asbjørnslett, B.E., 2012. Optimal fleet composition and periodic routing of offshore supply vessels. Eur. J. Oper. Res. 223 (2), 508–517.
Hoff, A., Andersson, H., Christiansen, M., Hasle, G., Løkketangen, A., 2010. Industrial aspects and literature survey: fleet composition and routing. Comput. Oper. Res. 37 (12), 2041–2061.
Kleywegt, A.J., Shapiro, A., Homem-de Mello, T., 2002. The sample average approximation method for stochastic discrete optimization. SIAM J. Optim. 12 (2), 479–502.
List, G.F., Wood, B., Nozick, L.K., Turnquist, M.A., Jones, D.A., Kjeldgaard, E.A., Lawton, C.R., 2003. Robust optimization for fleet planning under uncertainty. Transport. Res. Part E: Logist. Transport. Rev. 39 (3), 209–227.
Løkketangen, A., Woodruff, D., 1996. Progressive hedging and tabu search applied to mixed integer (0,1) multistage stochastic programming. J. Heurist. 2 (2), 111–128.
Meng, Q., Wang, T., 2010. A chance constrained programming model for short-term liner ship fleet planning problems. Maritime Policy Manage. 37 (4), 329–346.
Meng, Q., Wang, T., 2011. A scenario-based dynamic programming model for multi-period liner ship fleet planning. Transport. Res. Part E: Logist. Transport. Rev. 47 (4), 401–413.
Meng, Q., Wang, T., Wang, S., 2012. Short-term liner ship fleet planning with container transshipment and uncertain container shipment demand. Eur. J. Oper. Res. 223 (1), 96–105.
Meng, Q., Wang, T., Wang, S., 2015. Multi-period liner ship fleet planning with dependent uncertain container shipment demand. Maritime Policy Manage. 42 (1), 43–67.
Pantuso, G., Fagerholt, K., Hvattum, L.M., 2014a. A survey on maritime fleet size and mix problems. Eur. J. Oper. Res. 235 (2), 341–349.

Pantuso, G., Fagerholt, K., Wallace, S.W., 2014b. Solving hierarchical stochastic programs: application to the maritime fleet renewal problem. INFORMS J. Comput. 27 (1), 89–102.
Pantuso, G., Fagerholt, K., Wallace, Stein W., 2016. Uncertainty in Fleet Renewal: A Case from Maritime Transportation. Transport. Sci. 50 (2), 390–407. http://dx.doi.org/10.1287/trsc.2014.0566.
Papageorgiou, D.J., Nemhauser, G.L., Sokol, J., Cheon, M.-S., Keha, A.B., 2014. MIRPLib – a library of maritime inventory routing problem instances: survey, core model, and benchmark results. Eur. J. Oper. Res. 235 (2), 350–366.
Powell, W.B., 2011. Approximate Dynamic Programming: Solving the Curses of Dimensionality. John Wiley & Sons.
Powell, W.B., 2014. Clearing the jungle of stochastic optimization. INFORMS Tutorials in Operations Research: Bridging Data and Decision, 109–137.
Rockafellar, R.T., Uryasev, S., 2000. Optimization of conditional value-at-risk. J. Risk 2, 21–42.
Shapiro, A., Dentcheva, D., Ruszczynski, A., 2014. Lectures on Stochastic Programming: Modeling and Theory, vol. 16. SIAM.
Shapiro, A., Nemirovski, A., 2005. On complexity of stochastic programming problems. In: Continuous Optimization. Springer, pp. 111–146.
Shyshou, A., Gribkovskaia, I., Barceló, J., 2010. A simulation study of the fleet sizing problem arising in offshore anchor handling operations. Eur. J. Oper. Res. 203 (1), 230–240.
Singer, M., Donoso, P., Jara, S., 2002. Fleet configuration subject to stochastic demand: An application in the distribution of liquefied petroleum gas. J. Oper. Res. Soc. 53 (9), 961–971.
Stopford, M., 2008. Maritime Economics. Taylor & Francis, New York, NY.